

Multiscale quantile segmentation

LAURA JULIA VANEGAS*, MERLE BEHR† AND AXEL MUNK*,†

Institute for Mathematical Stochastics*,

University of Göttingen,

Max Planck Institute for Biophysical Chemistry†,

Göttingen, Germany,

and

Department of Statistics‡,

University of California at Berkeley, Berkeley, USA

Email:

[ljurava,munk}@math.uni-goettingen.de](mailto:{ljurava,munk}@math.uni-goettingen.de), behr@berkeley.edu

We introduce a new methodology for analyzing serial data by quantile regression assuming that the underlying quantile function consists of constant segments. The procedure does not rely on any distributional assumption besides serial independence. It is based on a multiscale statistic, which allows to control the (finite sample) probability for selecting the correct number of segments S at a given error level, which serves as a tuning parameter. For a proper choice of this parameter, this tends exponentially fast to the true S , as sample size increases. We further show that the location and size of segments are estimated at minimax optimal rate (compared to a Gaussian setting) up to a log-factor. Thereby, our approach leads to (asymptotically) uniform confidence bands for the entire quantile regression function in a fully nonparametric setup. The procedure is efficiently implemented using dynamic programming techniques with double heap structures, and software is provided. Simulations and data examples from genetic sequencing and ion channel recordings confirm the robustness of the proposed procedure, which at the same hand reliably detects changes in quantiles from arbitrary distributions with precise statistical guarantees.

Keywords: Change-points, Double heap, Dynamic programming, Multiscale methods, Quantile regression, Robust segmentation.

2010 Mathematics Subject Classification: 62G08, 62G15, 62G30, 62G35, 90C39.

1. Introduction

The analysis of serial data with presumably abrupt underlying distributional changes, for example, in its mean, median, or variance, is a long-standing issue and relevant to a magnitude of applications, e.g. to econometrics and empirical finance (Preuss et al., 2015; Shen, 2016; Russell and Rambaccussing, 2018), evolutionary and cancer genetics (Olshen et al., 2004; Liu et al., 2013; Zhang and Siegmund, 2007; Jónás et al., 2016; Futschik et al., 2014) or neuroscience (Cribben and Yu, 2017), to mention a few

(see Section 1.4 for a more comprehensive discussion). The present work proposes a new methodology for this task, denoted as *Multiscale Quantile Segmentation (MQS)* which on the one hand, is extremely robust as it does not rely on any distributional assumption (apart from independence) and on the other hand, still has high detection power with (even non-asymptotic) statistical guarantees.

More precisely, our methodology is based on quantile segments, i.e., quantile regression functions which are modeled as right-continuous piecewise constant functions ϑ with finitely but arbitrary many (unknown) segments S . We stress that even in such situations where the quantiles are not piecewise constant, this may serve as a reasonable proxy to cartoonize the quantile function in a simple but meaningful way. To fix our setting, we assume that the underlying regressor (e.g., time) is in the interval $[0, 1]$ and is sampled equidistantly at n sampling points $x_i := (i - 1)/n$. As our main results are nonasymptotic, extensions to general (ordered) sampling domains and non-equidistant sampling points are immediate. All such segment functions $\vartheta : [0, 1] \rightarrow \mathbb{R}$ are then comprised in the space

$$\Sigma = \left\{ \vartheta = \sum_{s=1}^S \theta_s \mathbf{1}_{[\tau_{s-1}, \tau_s)} : \theta_s \neq \theta_{s+1}, \ 0 = \tau_0 < \tau_1 < \dots < \tau_S = 1, \ S < \infty \right\}. \quad (1)$$

Hence, our quantile function consist of S (unknown) distinct segments with unknown segment values $\theta_s \in \mathbb{R}$ and segment lengths $\tau_s - \tau_{s-1}$ (see Figure 1.1 for illustration).

QSR-model (QUANTILE SEGMENT REGRESSION MODEL) Let $\beta \in (0, 1)$ and $\vartheta_\beta \in \Sigma$ a segment function. In the QSR-model one observes n independent random variables Z_i at equidistant sampling points $x_{i,n} = x_i = (i - 1)/n$ for $i = 1, \dots, n$ such that its β -quantiles are given as

$$\vartheta_\beta(x_i) = \inf\{\theta : \mathbf{P}(Z_i \leq \theta) = \beta\} \quad \text{for } i = 1, \dots, n. \quad (2)$$

Example 1.1. The first row of Figure 1.1 shows data Z_1, \dots, Z_n with $n = 2485$ from the QSR-model for three different quantiles $\beta = 0.25, 0.5, 0.75$. For example, the median is a segment function $\vartheta_{0.5} \in \Sigma$ (black line) with $S = 7$ segments. The data comes from 3 different distributional regimes. The first 350 observations are drawn from a normal distribution with variance 1, the next 1190 from a t distribution with 3 d.f. and variance 0.05 and the last 945 from a χ^2 distribution with 1 d.f. and variance 0.05. This scenario is covered by the QRS-model as only independence of the Z_i is assumed. Note that the QSR-model allows that different quantile curves may have entirely different segments, for example, the 0.25- and 0.75-quantile functions $\vartheta_{0.25}, \vartheta_{0.75}$ (gray lines) have an additional segment in the first regime ($S = 8$).

Our MQS-methodology in a nutshell: the second row in Figure 1.1 shows the MQS estimates (MQSE) for the median (red line) and the 0.25- and 0.75-quantiles (light red lines) for the data as in the first row. Together, we denote MQS' estimates for the 0.25, 0.5, and 0.75-quantiles as the multiscale segment boxplot (MSB). The third row shows the median and its MQSE together with a 90% simultaneous confidence band for the median (gray area) and simultaneous confidence intervals for the locations of the segment changes (blue intervals). The fourth and fifth rows show the corresponding plots for the 0.25 and 0.75 segment quantiles.

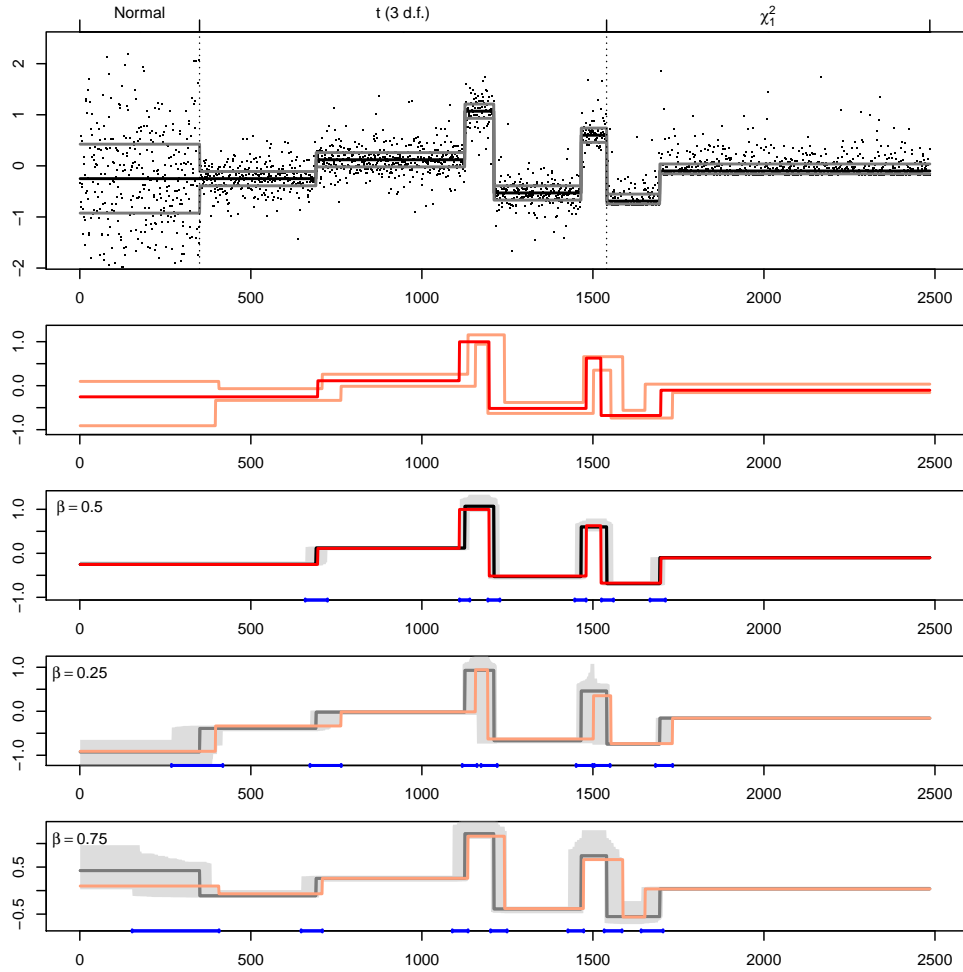


Figure 1.1: First row: Observations Z_1, \dots, Z_n , $n = 2485$, from Example 1.1 as in the QSR-model with median function $\vartheta_{0.5}$ (black line) and 0.25- and 0.75-quantile functions $\vartheta_{0.25}, \vartheta_{0.75}$ (grey lines). Data comes from three different distributional regimes: Normal, t_3 , and χ_1^3 (see Example 1.1). Second row: The multiscale box plot (MSB), with estimates (MQSE) for the median (red line), the 0.25- and 0.75-quantiles (light red lines), at nominal level $\alpha = 0.1$, see (8). Subsequent rows: True quantiles (black and grey solid lines) and MQSE (red and light red), together with 90% simultaneous confidence bands (grey area) and simultaneous confidence intervals for the change-point locations (blue intervals), for $\beta = 0.5, 0.75, 0.25$, respectively.

As illustrated in Example 1.1, the aim of this work is to provide a statistical methodology for multiscale quantile segmentation (MQS) in the general QSR-model. For each $\beta \in (0, 1)$, MQS provides estimates and confidence statements for:

1. the number S of segments $S(\vartheta_\beta)$,
2. the segment locations $\tau_1, \dots, \tau_{S-1} \in [0, 1)$,
3. and, based on these, the segment values, i.e., the quantiles $\theta_1, \dots, \theta_S \in \mathbb{R}$.

Our approach is based on a simple transformation: Given a candidate segment function $\vartheta \in \Sigma$ (which will depend on the data Z_i), we consider the transformed binary (pseudo) data

$$W_i = W_i(Z_i, \vartheta(x_i)) := \begin{cases} 0 & \text{if } \vartheta(x_i) - Z_i < 0, \\ 1 & \text{if } \vartheta(x_i) - Z_i \geq 0. \end{cases} \quad (3)$$

Note that if and only if the candidate function ϑ equals the true underlying regression function ϑ_β in the QSR-model, then W_1, \dots, W_n are i.i.d. Bernoulli distributed with success probability β . Based on this, our methodology “tests” in a multiscale fashion any possible candidate function in Σ to be valid: it selects a segment quantile function which does not contradict the i.i.d. Bernoulli assumption and, among those, has the smallest number of segments.

The unknown number and locations of segments of ϑ_β will be detected by a certain multiscale statistic $T_n(Z, \vartheta) = T_n(W(Z, \vartheta), \vartheta)$ (see (18)), which combines on intervals $[x_i, x_j]$ where $\vartheta|_{[x_i, x_j]}$ is constant (segments), with $1 \leq i \leq j \leq n$, the corresponding log-likelihood ratio tests for the hypothesis testing problems

$$H_{ij} : W_i, \dots, W_j \stackrel{i.i.d.}{\sim} B(\beta) \quad \text{vs.} \quad K_{ij} : W_i, \dots, W_j \stackrel{i.i.d.}{\sim} B(\beta') \text{ with } \beta' \neq \beta, \quad (4)$$

where $B(\beta)$ denotes a Bernoulli distribution with success probability β (see (18) for the precise definition of T_n). In a first step MQS determines the number of segments from the data given such $\beta \in (0, 1)$. For a given threshold $q \in \mathbb{R}$ (to be specified later), the estimated number of segments \hat{S} is the solution of a (non-convex) optimization problem with convex constraints given by the multiscale statistic T_n , namely

$$\hat{S} = \hat{S}(q) := \inf_{\vartheta \in \Sigma} \#J(\vartheta) \quad \text{s.t.} \quad T_n(W(Z, \vartheta), \vartheta) \leq q, \quad (5)$$

where $J(\vartheta)$ denotes the set of segments and $\#J(\vartheta)$ the number of segments of $\vartheta \in \Sigma$. That is, we choose the smallest number of segments such that the multiscale test $T_n(W(Z, \vartheta), \vartheta) \leq q$ still accepts. As, in a certain sense, this is a model selection step, we call \hat{S} the MQS selector of S . In a second step, we then constrain all candidate segment quantile functions to those with \hat{S} segments, that is, to the set

$$\mathcal{H}(q) := \{\vartheta \in \Sigma : \#J(\vartheta) = \hat{S}(q) \text{ and } T_n(W(Z, \vartheta), \vartheta) \leq q\}. \quad (6)$$

The MQS estimate (MQSE) $\hat{\vartheta}$ is then a particular simple segment function in $\mathcal{H}(q)$ based on the Wald-Wolfowitz runs tests (see Section 2 for details and Figure 1.1 for illustration).

1.1. Main results: Theory

For the MQSE $\hat{\vartheta}$, with ϑ_β being the true underlying regression function in the QSR-model, we immediately get from (5) that $\mathbb{P}(\hat{S}(q) > S) \leq \mathbb{P}(T_n(Z, \vartheta_\beta) \leq q)$. In Section 2.1 we show that $T_n(Z, \vartheta_\beta)$ can be bounded in distribution with a random variable $M_n = M_{n,\beta}$ that only depends on β and n and hence does not depend on ϑ_β or any other characteristics of the underlying distribution of the observations Z_i , namely

$$M_n := \max_{1 \leq i \leq j \leq n} \sqrt{2T_i^j(X, \beta) - P_{\ell,n}}, \quad (7)$$

where $X = (X_1, \dots, X_n)$ are i.i.d. Bernoulli distributed with mean β and a penalization $P_{\ell,n}$ depending only on n, i, j (see (18)). Therefore, for given n and β the finite sample-quantiles of M_n can be computed by Monte-Carlo simulations in a universal manner. Hence, choosing $q_n = q_n(\alpha)$ as the $(1 - \alpha)$ -quantile of M_n gives us control for the overestimation error of the number of segments included in our final estimator by a desired level α , namely

$$\mathbb{P}(\hat{S}_{n,\alpha} > S) \leq \alpha, \quad (8)$$

where $\hat{S}_{n,\alpha} := \hat{S}(q_n(\alpha))$. In Theorem 1.1 we present a refinement of this fact.

Theorem 1.1 (Overestimation error). *Consider the QSR-model. For $q = q_n(\alpha)$ as in (5) and (20) the MQS-selector $\hat{S}_{n,\alpha} := \hat{S}(q)$ satisfies uniformly over all segment functions $\vartheta \in \Sigma$*

$$\mathbb{P}(\hat{S}_{n,\alpha} > S + s) \leq \alpha^{\lfloor s/2 \rfloor + 1}, \quad (9)$$

where $\lfloor \cdot \rfloor := \max\{m \in \mathbb{Z} : m \leq x\}$, for all $x \in \mathbb{R}$, i.e. the floor function.

This means, in addition to controlling the overall overestimation error ($s = 0$), the error of overestimating the number of segments by more than s decays exponentially fast. This reveals that changes detected by MQS are, with very high probability, indeed present in the signal. Therefore, α controls the false positives in a strong family-wise error sense.

The overestimation bound in Theorem 1.1 will be complemented by an explicit bound for the underestimation error, see Theorem 1.2 in the following. Together, this allows for precise fine-tuning of the error of a wrong number of detected segments via the choice of the error level α . Clearly, such an underestimation bound for $\mathbb{P}(\hat{S}_{n,\alpha} < S)$ has to depend on some characteristics of the function ϑ_β , specifically on the length and height of the jumps, as no method can detect arbitrary small changes for a fixed number of data. Moreover, note that even a large jump of ϑ_β is not identifiable from the QSR-model, if it does not induce a sufficiently large jump in the respective distribution functions, as the following example shows.

Example 1.2. *For sufficiently large $L > 0$ and small $\epsilon > 0$ consider random variables X, Y such that $\mathbf{P}(X = L) = 0.5$, $\mathbf{P}(X = -L) = 0.5 - \epsilon$, $\mathbf{P}(X = -L + \epsilon) = \epsilon$ and $\mathbf{P}(Y = -L) = 0.5 - \epsilon$, $\mathbf{P}(Y = L) = 0.5$, $\mathbf{P}(Y = L - \epsilon) = \epsilon$, as in Figure 1.2 (left).*

Then, if half of the sample comes from X , i.e., $Z_1, \dots, Z_{n/2} \sim X$ and the other half from Y , i.e., $Z_{n/2+1}, \dots, Z_n \sim Y$ as in the QSR-model, the underlying median regression function $\vartheta_{0.5}$ (blue line) has a large jump of size $2L-2\epsilon$ at $\tau = 0.5$. However, for sufficiently small ϵ (depending on n), because the probability of sampling $-L+\epsilon$ or $L-\epsilon$ is very small, this jump is not detectable from the observations Z_1, \dots, Z_n , see Figure 1.2 (right).

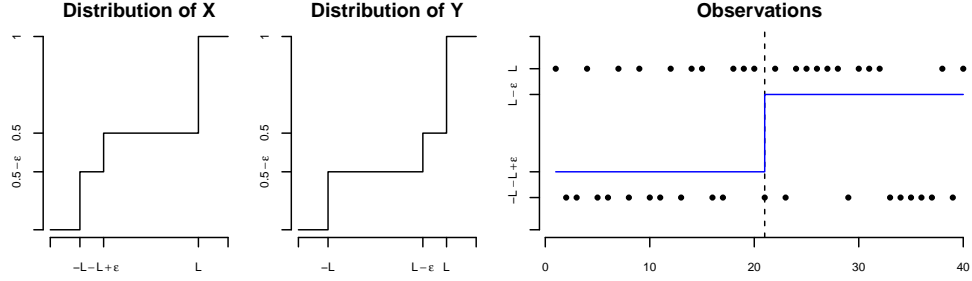


Figure 1.2: Left: Cumulative distribution function of X and Y as in Example 1.2. Right: Independent observations $Z_1, \dots, Z_{20} \sim X$ and $Z_{21}, \dots, Z_{40} \sim Y$ together with a median regression function (blue line) as in the QSR-model. Here $n = 40$, $L = 1$, and $\epsilon = 0.01$.

The following definition specifies situations where a quantile segment is detectable.

Definition 1.1 (Quantile Jump Function). *For a distribution function F and $\beta \in (0, 1)$, let $\theta_\beta := \inf\{\theta : F(\theta) \geq \beta\}$ be the β -quantile. Then the quantile jump function $\xi_{F,\beta} : \mathbb{R} \rightarrow [0, 1]$ is defined as*

$$\xi_{F,\beta}(\delta) = |F(\theta_\beta + \delta) - \beta|.$$

The quantile jump function quantifies how much a *quantile jump* in the QSR-model influences data around a jump. This is specified by a homogeneity condition, namely that around each jump τ_s , $s = 1, \dots, S-1$, there exist intervals $[\tau_s - \lambda_s, \tau_s]$ and $[\tau_s, \tau_s + \lambda_s]$, for some $\lambda_s \in (0, 1)$, such that samples of points from those intervals are not just independent but also identically distributed.

LHD-condition (LOCALLY HOMOGENEOUS DISTRIBUTIONS) For $\vartheta_\beta \in \Sigma$, $n \in \mathbb{N}$, and Z_1, \dots, Z_n as in the QSR-model assume that for $s = 1, \dots, S-1$

$$Z_{\lceil n(\tau_{s-1} - \lambda_s) + 1 \rceil}, \dots, Z_{\lfloor n\tau_s \rfloor} \stackrel{i.i.d.}{\sim} F_s^- \quad \text{and} \quad Z_{\lceil n\tau_s + 1 \rceil}, \dots, Z_{\lfloor n(\tau_s + \lambda_s) \rfloor} \stackrel{i.i.d.}{\sim} F_s^+,$$

for some distribution functions $F_1^-, \dots, F_{S-1}^-, F_1^+, \dots, F_{S-1}^+$ and $\lambda_1, \dots, \lambda_s \in (0, 1]$.

Note that this condition is still very general, allowing distributional changes inside segments, as well as at jumps, as seen in Example 1.1. We will show that under the LHD-condition one can bound the probability for the MQSE to underestimate the

number of segments in terms of the minimal quantile jump and the minimal length of constant distribution segments,

$$\Xi := \min_{s=1,\dots,S} \min \left\{ \xi_{F_s^-, \beta}(\theta_s - \theta_{s-1}), \xi_{F_s^+, \beta}(\theta_{s-1} - \theta_s) \right\} \quad \text{and} \quad \Lambda := \min_{s=1,\dots,S} \lambda_s. \quad (10)$$

In Theorem 2.1 we show a general exponential bound for underestimating the number of segments by the MQSE, which provides the following result.

Theorem 1.2. *Consider the QSR-model with the LHD-condition, $\hat{S}_{n,\alpha}$ as in (8), and Λ, Ξ as in (10). Then, for $q_n(\alpha) > 0$ the $1 - \alpha$ quantile of M_n in (7), it holds that*

$$\mathbb{P} \left(\hat{S}_{n,\alpha} < S \right) \leq 4(S-1) e^{-n\Lambda\Xi^2} \left[e^{2\sqrt{n\Lambda\Xi}(q_n(\alpha)/\sqrt{2} + \sqrt{\log(2e/\Lambda)})} + 1 \right]. \quad (11)$$

Note that whenever $\beta \rightarrow 0$ or $\beta \rightarrow 1$ then $\Xi \rightarrow 0$ and hence, the bound on the r.h.s. in (11) becomes trivial. This reflects the fact that for very high or very small quantiles it is arbitrarily difficult to capture changes from finitely many samples.

Combining (8) and (11), we obtain an explicit bound for estimating the number of segments correctly, depending on α, n, Λ and Ξ in (23), namely,

$$\mathbb{P} \left(\hat{S}_{n,\alpha} = S \right) \geq 1 - \alpha(q_n) - 4(S-1) e^{-n\Lambda\Xi^2} \left[e^{2\sqrt{n\Lambda\Xi}(q_n/\sqrt{2} + \sqrt{\log(2e/\Lambda)})} + 1 \right], \quad (12)$$

uniformly over all possible segment functions in Σ satisfying (10). As $\alpha(q_n)$ converges to zero as $q_n \rightarrow \infty$ (see Section 2), the MQS selector is consistent, that is $\mathbb{P} \left(\hat{S}_{n,\alpha} = S \right) \rightarrow 1$ as $n \rightarrow \infty$, whenever the threshold parameters are chosen such that $q_n \rightarrow \infty$ and $q_n/\sqrt{n} \rightarrow 0$. Moreover, q_n can be chosen such that the r.h.s of (12) is maximized leading to exponentially fast selection consistency.

In Theorem 2.2 we refine these consistency results to the situation where $\Xi = \Xi_n$ and $\Lambda = \Lambda_n$ vanish as $n \rightarrow \infty$. We give a sharp condition on Ξ_n, Λ_n, q_n under which MQS consistently estimates the number of segments S and show that (up to constants) these conditions cannot be improved, in general.

With the choice of $q_n = q_n(\alpha)$ as in (8), the multiscale approach of MQS directly yields (asymptotically) honest simultaneous confidence bands for the underlying regression function ϑ_β and simultaneous confidence intervals for the change-points τ via the set $\mathcal{H}(q_n)$ in (6), see last three plots of Figure 1.1 and Remark 2.5 for further details.

Besides model selection consistency and confidence statements for all quantities, the MQS procedure also yields minimax optimal estimation rates (up to a log-factor) for the change point locations. In Theorem 2.3 we show that whenever $q_n = o(\sqrt{\log(n)})$ and $\Lambda_n^{-1} = o(n/\log(n))$ then for any $\Xi_0 > 0$

$$\sup_{\substack{\vartheta \in \Sigma \\ \Lambda > \Lambda_n, \Xi > \Xi_0}} \mathbb{P} \left(\max_{\tau \in J(\vartheta)} \min_{\hat{\tau} \in J(\hat{\vartheta}(q))} |\hat{\tau} - \tau| > \frac{\log(n)}{n} \frac{1}{\Xi^2} \right) \rightarrow 0, \quad (13)$$

where the minimax rate is lower bounded by the sampling rate $1/n$ and hence, the rate in (13) is optimal (up to the log-factor).

1.2. Implementation

It has been exploited for a long time that global optimization procedures to detect segment changes in parametric models (mainly Gaussian), can be computed efficiently using dynamic programming, see e.g., (Bellman, 1954; Bai and Perron, 1998; Kempe et al., 2008; Boysen et al., 2009; Killick et al., 2012; Davies et al., 2012; Frick et al., 2014; Zou et al., 2014; Pein et al., 2017; Haynes et al., 2017; Celisse et al., 2018; Ruggieri, 2018; Wang et al., 2018). However, the exact computation of the nonparametric quantile segments of the MQSE in (5) leads to an additional computational burden compared to the case where the underlying jump signal corresponds to a parameter of a specific data distribution. Whereas the parametric case typically involves updating a running mean, which can be done in $\mathcal{O}(1)$ time, the quantile case involves updating the empirical quantile, which depends on the ordering of the data and hence, is computationally more involved. We incorporate an efficient running quantile computation as described in (Astola and Campbell, 1989), which is based on double heap structures. Thereby, the worst case computation time of MQSE only increases by a log-factor compared to the parametric case, as e.g., discussed in (Frick et al., 2014), being of the order $\mathcal{O}(n^2 \log n)$. However, in many situations, depending on the underlying signal, the actual complexity will be almost linear. We give more details on the implementation of MQSE in Section 3. An R package `mqe` is available at http://www.stochastik.math.uni-goettingen.de/mqe_1.0.tar.gz.

1.3. Simulation results and data examples

In Section 4 we explore the MQS procedure in a comprehensive simulation study, including a comparison with several other state of the art segmentation methods, which have been designed to be robust, namely R-FPOP (Fearnhead and Rigaill, 2017), WBS (Fryzlewicz, 2014), HSMUCE (Pein et al., 2017), and QS (Eilers et al., 2005). In order to compare the detection power of MQSE in a benchmark scenario, we also compare with SMUCE (Frick et al., 2014) which is tailored to normal data. A major finding is that while other methods only work well in some specific cases, MQS reliably detects changes in the quantiles for arbitrary distributions.

Figure 1.3 illustrates a benchmark scenario which shows data similar as in Example 1.1, together with the MQS, SMUCE, R-FPOP, WBS, HSMUCE, and QS estimators (red lines) for the median or mean respectively. Compared to Figure 1.1 in Figure 1.3 variances have been doubled and in the second regime the degrees of freedom of the t -distribution lowered to d.f.= 1 (Cauchy). More precisely, the first 350 observations are drawn from a normal distribution with variance 2, the next 1190 from a t distribution with 1 d.f. and variance 0.1 and the last 945 from a χ^2_1 distribution with 1 d.f. and variance 0.1 (compare with Figure 1.1). MQS turns out to have good detection power (first regime), to be robust to heavy tails (second regime), change in variance, and more generally to arbitrary distributional variations and skewness (third regime). In contrast, SMUCE (specifically designed for gaussian error with homogeneous variance) is very sensitive to changes in variance and heavy-tailed distributions, adding a lot of artificial changes in those cases. WBS is more robust to high variances, but also

adds artificial changes in the presence of outliers. R-FPOP is robust to heavy-tailed distributions, but is susceptible to changes in variance, adding artificial changes in the first 350 observations. On the contrary, HSMUCE and QS suffer from oversmoothing and miss important data features. In this case, MQSE is capable of exploring the concentration of points around the median from the heavy-tailed t (1 d.f.) distribution, despite low signal to noise ratio.

Recall that MQS does not just provide some reconstruction of the underlying β -quantile, but it also comes with precise statistical guarantees, such as honest confidence statements. This is particularly valuable for many real data examples, where there is uncertainty about the precise observational distribution. We demonstrate this in Figure 1.4 which shows an example from cancer genetics, see Behr et al. (2018), where one aims to detect copy-number aberrations (changes in the number of copies of certain regions of the genome) in tumor DNA (see Section 5 for details and a further data set on ion channel recordings). Here, the MQS procedure proves to be particularly valuable (see Subsection 5.1 for details). While most of the other methods include artificial jumps in their reconstruction (which in this data example are known to be not present in the underlying signal and result from sequencing artifacts, see Section 5.1 for details), MQS reliably recovers most of the copy-number aberrations correctly. Moreover, copy-number aberrations are known to often omit heterogeneity on different segments, and MQS adds a powerful visualization tool for this via the multiscale box plot.

1.4. Related work

The estimation of step functions with unknown number and location of segments are widely discussed problems; we mention (Olshen et al., 2004; Fearnhead, 2006; Tibshirani and Wang, 2008; Spokoiny, 2009; Boysen et al., 2009; Harchaoui and Lévy-Leduc, 2010; Jeng et al., 2010; Killick et al., 2012; Niu and Zhang, 2012; Siegmund, 2013; Frick et al., 2014; Matteson and James, 2014; Fryzlewicz, 2014; Du et al., 2016; Fryzlewicz, 2018) for a variety of methods and related statistical theory.

Methods for segment regression problems that offer statistical guarantees in terms of minimax optimal estimation rates, typically concern the mean function assuming normality, see e.g., (Harchaoui and Lévy-Leduc, 2010; Cai and Xiong, 2012; Fryzlewicz, 2014; Li et al., 2016; Pein et al., 2017). In contrast, we target the quantile function (see e.g., Koenker (2005) for a survey) and do not assume a specific distributional model, besides independence and the LHD-condition. We stress, however, that extensions for serially dependent data appear doable to us and will be postponed to future work.

Mostly related to our work are methods which explicitly aim to provide robust methodology for segmentation. From a general perspective, segment regression may be considered as a particular case of a high dimensional linear model, with a very specific design matrix. Belloni and Chernozhukov (2011) consider sparse high dimensional quantile regression and show that minimizing the asymmetric absolute deviation loss together with L_1 penalization yields almost optimal estimation rates (in L_1 loss). However, their results require certain regularity conditions on the design matrix (similar to restricted eigenvalue conditions) which are not fulfilled for the specific design which

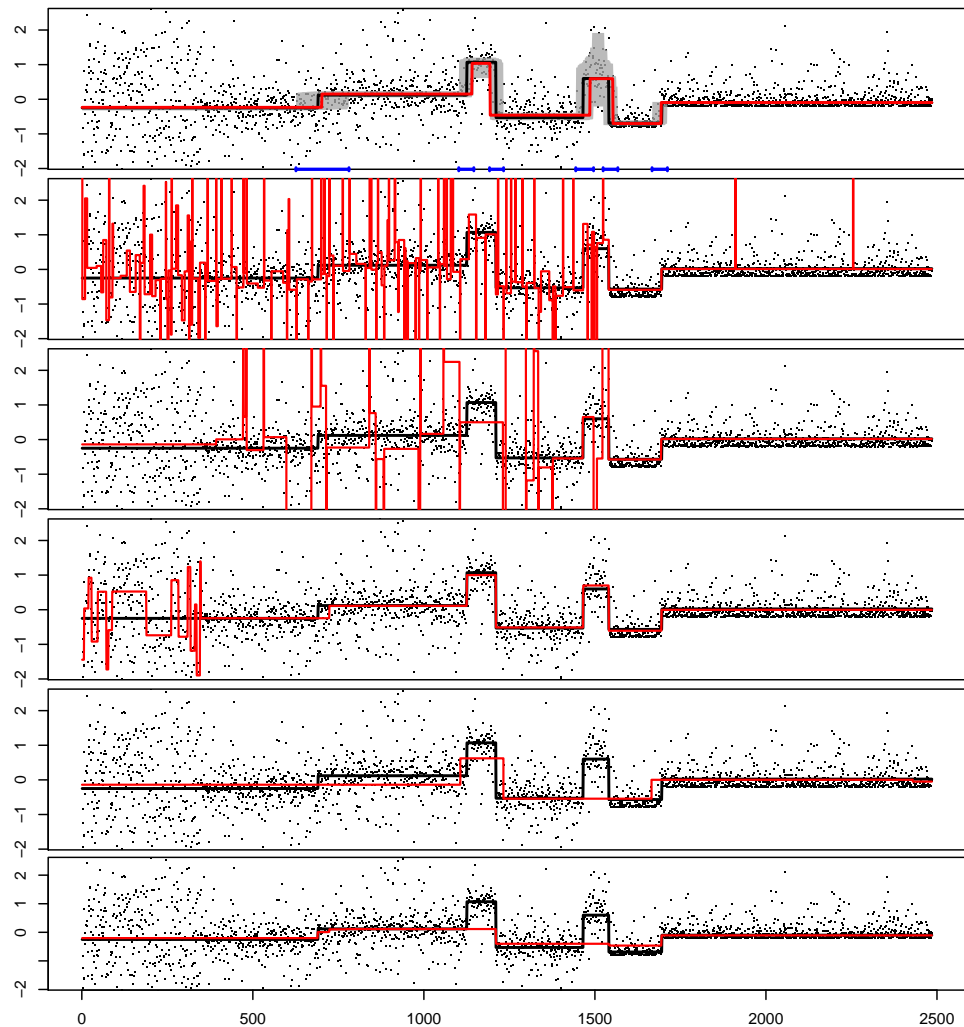


Figure 1.3: Observations Z_1, \dots, Z_n , $n = 2485$ (black dots) analog as in Example 1.1 with different variances and 1 degree of freedom for the t distribution (see main text for details) together with true median regression function (black lines). From top to bottom (red lines): MQSE for the median with confidence band (grey area) for $\alpha = 0.1$ and confidence intervals (blue intervals), SMUCE (Frick et al., 2014), WBS (Fryzlewicz, 2014), R-FPOP (Fearnhead and Rigaill, 2017), HSMUCE (Pein et al., 2017) and QS (Eilers et al., 2005).

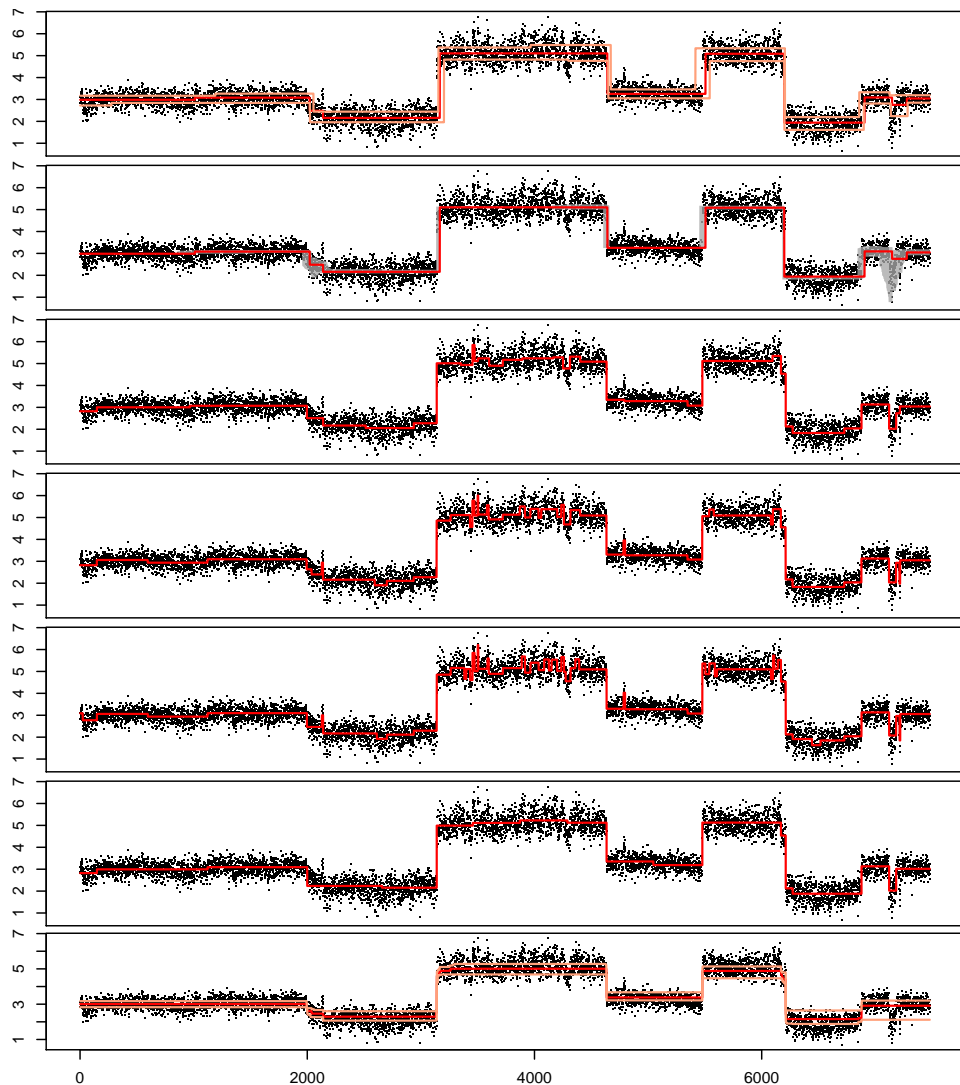


Figure 1.4: Preprocessed WGS data (black dots) of cell line LS411 from colorectal cancer and different estimates for the underlying CNA's (red lines). Sequencing was performed by Complete Genomics in collaboration with the Wellcome Trust Centre for Human Genetics at the University of Oxford. From top to bottom: MQS multiscale box plot with $\alpha = 0.01$, MQSE for the median with confidence band for $\alpha = 0.01$, SMUCE (Frick et al., 2014), WBS (Fryzlewicz, 2014), R-FPOP (Fearnhead and Rigaill, 2017), HSMUCE (Pein et al., 2017) and QS (Eilers et al., 2005) (estimated 0.25, 0.5, and 0.75 quantiles).

corresponds to a multiscale segmentation setting. Eilers et al. (2005); Li and Zhu (2007) consider minimizing absolute loss with an L_1 -penalty for quantile regression for the segment regression setting, while not providing any theoretical results. More generally, Duembgen and Kovac (2009) consider quantile regression via minimizing a convex loss with a total variation penalty and provide certain consistency results. In contrast, MQS uses the transformation (3) which is closely related to residual signs as used in Dümbgen (1998) for goodness-of-fit testing and ? for taut string estimation. Finally, Aue et al. (2014, 2017) consider quantile segmentation in a time series context based on a minimum description length criterion to select the number of segments and show consistency of their method, whereas in our (simpler) setting we obtain exponentially fast selection consistency, see (12).

The previously mentioned methods that target quantile regression do not come with specific confidence statements as MQS does. Conceptually, this is closely related to confidence bands and intervals in the context of change point regression introduced in Frick et al. (2014) for general exponential families. The present methodology extends this to the situation where no parametric model has to be assumed.

2. Theory

In Section 2.1 we introduce the MQS methodology in more details, in Section 2.2 we introduce the MQSE, and in Section 2.3 we present our results on model selection consistency, confidence statements, and minimax optimal estimation rates for MQS. Proofs are postponed to the Appendix. We start with a discussion of the model assumptions.

At first glance, it might seem restrictive that the QSR-model requires for the underlying β -quantile regression function ϑ_β that $\mathbf{P}(Z_i \leq \vartheta_\beta(x_i)) = \beta$ (and not, more generally, that $\vartheta_\beta(x_i) = \inf\{\theta : \mathbf{P}(Z_i \leq \theta) \geq \beta\}$). However, such assumption is unavoidable for efficient (i.e., with non-trivial power) control of overestimation of the number of segments, as it is achieved by the proposed method, without assuming a specific observational distribution. To see this, note that without making any distributional assumptions, for given independent observations Z_1, \dots, Z_n and candidate quantiles $\vartheta(x_1), \dots, \vartheta(x_n)$, all information from Z_i about the candidate ϑ is captured in the transformation $W_i = W_i(Z_i, \vartheta(x_i))$, $i = 1, \dots, n$ in (3). Now assume that in the QSR-model the condition in (2) is replaced by

$$\vartheta_\beta(x_i) = \inf\{\theta : \mathbf{P}(Z_i \leq \theta) \geq \beta\}. \quad (14)$$

Consider some (discontinuous) distribution function F for which (14) and (2) differ, such that there exists $\theta_0 \in \mathbb{R}$ with $F(\theta_0) = 1$ and $\lim_{x \nearrow \theta_0} F(x) < \beta$. Consider observations in the QSR-model with $Z_1, \dots, Z_n \stackrel{i.i.d.}{\sim} F$. Then, the true β -quantile ϑ_β is constant with $\vartheta_\beta \equiv \theta_0$ and for any data Z_i the transformation in (3) with truth ϑ_β yields $W_i = W_i(Z_i, \theta_0) = 1$ for $i = 1, \dots, n$. However, for any other data Z_i the constant candidate $\vartheta \equiv \theta_0$ with $\theta_0 \geq \max(Z_i)$, results in exactly the same transformation $W_i = W_i(Z_i, \theta_0) = 1$ for $i = 1, \dots, n$. Consequently, if one allows in

the QSR-model for generalized quantiles as in (14) controlling segment overestimation as in Theorem 1.1 appears too ambitious, as it rules out any reasonable estimator, i.e., this can only be achieved when setting $S = 0$ always. In fact, quantile estimation of non continuous distributions is well known to require more specific model assumptions in general, see e.g. (Machado and Silva, 2005). The MQS procedure allows quantile regression for discrete distributions, as long as the assumptions of the QSR-model hold.

2.1. Multiscale procedure

Given β , observations $Z = (Z_1, \dots, Z_n)$ from QSR-model and a function $\vartheta \in \Sigma$ with S segments as in (1) (which may depend on the data Z_i), the MQS methodology is based in a first step on a multiscale test to decide whether or not ϑ is a good candidate for the underlying unknown quantile function ϑ_β . To this end, fix an interval $[x_i, x_j] \subseteq [\tau_{s-1}, \tau_s]$ for some $1 \leq s \leq S$, that is, an interval where the candidate function ϑ is constant with value θ_s . When the true quantile function ϑ_β is constant on $[x_i, x_j]$ as well, the decision problem of whether or not ϑ coincides with the truth on the interval $[x_i, x_j]$ translates to the hypothesis testing problem

$$\begin{aligned} H_{ij} : & \mathbb{P}(Z_k \leq \theta_s) = \beta \text{ for all } i \leq k \leq j \\ K_{ij} : & \mathbb{P}(Z_k \leq \theta_s) \neq \beta \text{ for all } i \leq k \leq j. \end{aligned} \quad (15)$$

Equivalently, one can write (15) using the transformed data in (3) as the hypothesis testing problem in (4). The log-likelihood-ratio test for the hypothesis testing problem (4) and (15), respectively, is given by the test statistic

$$\begin{aligned} T_i^j(W) &= T_i^j(W(Z, \theta_s)) = \log \left(\frac{\sup_{\beta'} \prod_{l=i}^j f_{\beta'}(W_l)}{\prod_{l=i}^j f_\beta(W_l)} \right) \\ &= (j - i + 1) \left(\bar{W}_i^j \log \left(\frac{\bar{W}_i^j}{\beta} \right) + (1 - \bar{W}_i^j) \log \left(\frac{1 - \bar{W}_i^j}{1 - \beta} \right) \right), \end{aligned} \quad (16)$$

where $f_\beta(x) = \beta^x(1 - \beta)^{1-x}$ denotes the probability mass function of the Bernoulli distribution and $\bar{W}_i^j := (j - i + 1)^{-1} \sum_{l=i}^j W_l$. That is, the test is then of the form

$$\Phi_{ij}(Z) = \begin{cases} 0 & \text{if } \sqrt{2T_i^j(W(Z, \theta_s))} \leq q_{i,j}, \\ 1 & \text{otherwise,} \end{cases} \quad (17)$$

where the threshold $q_{i,j} := q_{i,j}(\alpha)$ determines the level α of the test (note that, under H_{ij} the distribution of $T_i^j(W)$ is independent of ϑ_β). However, we do not know where and on which scales the true ϑ_β is constant and thus, we have to consider all intervals on all different scales simultaneously. This means that a candidate function ϑ is accepted if and only if it gets accepted by all local tests Φ_{ij} in (17), for appropriately chosen

thresholds q_{ij} . More precisely, define the penalized multiscale statistic (as a functional on Σ) as

$$T_n(Z, \bullet) := \max_{\substack{1 \leq i \leq j \leq n \\ \bullet \text{ is constant on } [x_i, x_j]}} \sqrt{2T_i^j(W(Z, \bullet), \beta)} - P_{\ell, n}. \quad (18)$$

with $P_{\ell, n} := \sqrt{2 \log(\epsilon n / \ell)}$, where $\ell = j - i + 1$ denotes the scale. For some given threshold $q = q_n(\alpha)$ a candidate function ϑ is accepted if and only if $T_n(Z, \vartheta) \leq q_n(\alpha)$. This means that we choose local thresholds $q_{ij}(\alpha)$ in (17) as introduced in (Dümbgen and Spokoiny, 2001; Dümbgen and Walther, 2008; Frick et al., 2014) of the form

$$q_{ij}(\alpha) = q_n(\alpha) + P_{\ell, n}, \quad (19)$$

where $\ell = j - i + 1$ denotes the scale.

Remark 2.1. *A heuristic reasoning for the particular penalization $P_{\ell, n}$ in (18) is as follows. In order to put different scales on equal footing, one has to choose larger thresholds for smaller scales. On the other hand, it follows from Wilk's theorem (see (Frick et al., 2014) for a more precise argument) that for sufficiently large intervals the local statistics $\sqrt{2T_i^j}$ are well approximated by the absolute value of a standard normal. As the maximum of ℓ/n independent standard normals grows as $\sqrt{2 \log(\ell/n)}$, the particular choice in (19) ensures that $T_n(Z, \bullet)$ in (18) remains finite even when $n \rightarrow \infty$ for any fixed $\alpha \in (0, 1)$.*

Note that for $X = (X_1, \dots, X_n)$ i.i.d. Bernoulli distributed with mean β and $\vartheta = \vartheta_\beta$, the statistic $T_n(Z, \vartheta_\beta)$ in (18) follows the same distribution as

$$\max_{\substack{1 \leq i \leq j \leq n \\ \vartheta_\beta \text{ is constant on } [x_i, x_j]}} \sqrt{2T_i^j(X, \beta)} - P_{\ell, n},$$

which is bounded by M_n in (7) in probability. The distribution of M_n does not depend on any characteristics of the unknown ϑ_β and hence, we can determine its quantiles via Monte-Carlo simulations. Thus, we can define $q_n(\alpha)$ as the $(1 - \alpha)$ -quantile of M_n , i.e.,

$$q_n(\alpha) := \inf\{q : \mathbb{P}(M_n \leq q) \geq 1 - \alpha\}. \quad (20)$$

This choice guarantees that the true quantile function ϑ_β gets accepted by the above testing procedure with probability at least $1 - \alpha$, which leads to confidence statement for all quantities of ϑ_β , see Remark 2.5. In the next section we now define the MQS estimator (MQSE) for ϑ_β , which selects a specific candidate function accepted by the above testing procedure, namely, an element in $\mathcal{H}(q_n(\alpha))$ as in (6).

Remark 2.2. *It is shown in (Frick et al., 2014; Dümbgen and Spokoiny, 2001) that M_n converges in distribution to an almost surely finite random variable M (which is, indeed, independent of β). Note that for any $\alpha \in (0, 1)$ this implies $\limsup_n q_n(\alpha) < \infty$.*

2.2. MQS estimator (MQSE)

In contrast to parametric models (see (Frick et al., 2014)), since we do not make any assumptions on the specific distribution of the observations Z_i in the QSR-model, (local) maximum likelihood methods cannot be directly applied. In the following, we present an approach which uses the transformed data in (3) and is based on the Wald-Wolfowitz runs statistic (Wald and Wolfowitz, 1940). Recall that, for $\vartheta = \vartheta_\beta$ the true underlying regression function in (3), the transformed observations W_1, \dots, W_n are i.i.d. Bernoulli distributed with mean β . Let R be the number of runs of the sequence W_1, \dots, W_n , i.e.,

$$R(W) := \#\{1 \leq i \leq n-1 : W_i \neq W_{i+1}\} + 1,$$

and $N_0(W) := \sum_{i=1}^n W_i$. Then, conditioned on $N_0 = n_0$ and $n - N_0 = n_1$, it holds that R is asymptotically normally distributed with mean $\mu = 2n_1 n_0 / n - 1$ and variance $\sigma^2 = 2n_1 n_0 (2n_1 n_0 - n) / (n^2(n-1))$ see (Wald and Wolfowitz, 1940). Hence, for $\vartheta = \vartheta_\beta$ in (3) it follows that $\mathbf{P}(R(W) = r, N_0(W) = k) = \mathbf{P}(R(W) = r, | N_0(W) = k) \mathbf{P}(N_0(W) = k)$ is asymptotically well approximated by

$$D(r, k) := \binom{n}{k} \frac{\beta^k (1-\beta)^{n-k}}{\sqrt{2\pi\sigma^2}} \exp\left(-\frac{(r - \mu(n, k))^2}{2\sigma(n, k)^2}\right). \quad (21)$$

Definition 2.1 (MQSE). *For some threshold value $q > 0$, the MQS estimator is defined via $\mathcal{H}(q)$ in (6) as*

$$\hat{\vartheta} \in \operatorname{argmax}_{\vartheta \in \mathcal{H}(q)} D(R(W(Z, \vartheta)), N_0(W(Z, \vartheta))).$$

Remark 2.3. Note that the estimator MQSE may not be unique, as for two estimators $\hat{\vartheta}, \tilde{\vartheta} \in \mathcal{H}(q)$ it is possible that $R(\hat{W}) = R(\tilde{W})$ and $N_0(\hat{W}) = N_0(\tilde{W})$, for $\hat{W} := W(Z, \hat{\vartheta})$ and $\tilde{W} := W(Z, \tilde{\vartheta})$ as in (3). For n sufficiently large, we found it to be unique in most of the cases. When it is not unique we choose the first feasible change point location.

Remark 2.4. Another possible choice of estimator in $\mathcal{H}(q)$ is to minimize the asymmetric absolute deviation loss

$$\hat{\vartheta} := \operatorname{argmin}_{\hat{\vartheta} \in \mathcal{H}(q)} \sum_{i=1}^n (Z_i - \hat{\vartheta}(x_i)) (\beta - \mathbb{1}_{\{Z_i < \hat{\vartheta}(x_i)\}}), \quad (22)$$

as, for example, also considered in (Eilers et al., 2005; Li and Zhu, 2007; Duembgen and Kovac, 2009; Belloni and Chernozhukov, 2011). However, we found the estimator in Definition 2.1 to perform better in practice. We stress, however, that our theoretical results in Section 2.3 hold true for any choice in $\mathcal{H}(q)$, in particular, also for (22).

2.3. Consistency results

From the construction of the MQSE $\hat{\vartheta}$ it follows with $q_n(\alpha)$ as in (20), that the corresponding number of segments does not exceed the true number of segments at given

error level α , as described in equation (8) and Theorem 1.1. As already argued in Section 1, any bound on the underestimation error must depend on further characteristics of the underlying quantile function ϑ_β and on the respective quantile jumps for the distributions $F_1^-, \dots, F_S^-, F_1^+, \dots, F_S^+$ in the LHD-condition (recall Example 1.2 and Definition 1.1). To this end, let

$$\xi_s := \min \{\xi_{F_s, \beta}(\delta_s), \xi_{F_s, \beta}(-\delta_s)\} \quad s = 1, \dots, S, \quad (23)$$

with $\delta_s = \theta_s - \theta_{s-1}$ and for $q > 0$ and λ_s as in the LHD-condition. Let

$$\gamma_{n,s}(q) = \left(1 - 2 \exp \left(- \frac{\left(\sqrt{2n\lambda_s} \xi_s - q - \sqrt{2 \log(2e/\lambda_s)} \right)_+^2}{2} \right) - 2 \exp(-n\lambda_s \xi_s^2) \right)^2. \quad (24)$$

Theorem 2.1 (Underestimation error). *Consider the QSR-model together with the LHD-condition and $\hat{S}(q)$ as in (5). Then, for $q > 0$*

$$\mathbb{P}(\hat{S}(q) \geq S) \geq \prod_{s=1}^S \gamma_{n,s}(q).$$

From Theorem 2.1 we obtain that for any fixed $q > 0$ and $\Lambda, \Xi > 0$ in (10) the probability of underestimating the number of segments vanishes exponentially fast, see Theorem 1.2.

Remark 2.5 (Confidence statements). *From Theorem 1.2 it follows easily that the set $\mathcal{H}(q_n(\alpha))$ in (6) with $q_n(\alpha)$ as in (20) constitutes an asymptotically honest $(1 - \alpha)$ -confidence band for ϑ_β in the QSR-model with the LHD-condition uniformly over segment functions with minimal Λ and Ξ in (23). It follows from Remark 2.2 and Theorem 2.1 for $\Lambda_0 > 0$ and $\Xi_0 > 0$, that for any $\alpha \in (0, 1)$ as $n \rightarrow \infty$*

$$\begin{aligned} \inf_{\substack{\vartheta \in \Sigma: \\ \Lambda > \Lambda_0, \Xi > \Xi_0}} \mathbb{P}(\vartheta_\beta \in \mathcal{H}(q_n(\alpha))) &\geq \mathbb{P}(T_n(Z, \vartheta_\beta) \leq q_n(\alpha)) - \mathbb{P}(\hat{S}(q) < S) \\ &\geq 1 - \alpha - \mathbb{P}(\hat{S}(q) < S) \geq 1 - \alpha + o(1). \end{aligned}$$

$\mathcal{H}(q)$ can be computed easily simultaneously with the MQS estimator $\hat{\vartheta}$ (see Section 3). Further, as explained in (Frick et al., 2014), from $\mathcal{H}(q_n(\alpha))$ confidence intervals for the segment locations τ and for the quantile values θ can be constructed.

From Theorems 1.2 and the fact that if $q_n \rightarrow \infty$, $\alpha_n := \mathbf{P}(M_n > q_n) \rightarrow 0$, it follows directly that for any fixed $\Lambda, \Xi > 0$ and some sequence $q_n \rightarrow \infty$ such that $q_n/\sqrt{n} \rightarrow 0$ MQS performs consistent model selection for the number of c.p.'s. The following result goes beyond this and considers the situation of a sequence of regression function $\vartheta_\beta(n)$ in the QSR-model, where the minimal scale $\Lambda = \Lambda_n$ and the minimal quantile jump $\Xi = \Xi_n$ can vanish as $n \rightarrow \infty$.

Theorem 2.2 (Model selection consistency). *For a sequence $\vartheta_{\beta,n} \in \Sigma$ with Λ_n and Ξ_n as in (10), consider the QSR-model with the LHD-condition and $\hat{S}(q)$ as in (5). For some sequence $q_n \rightarrow \infty$, assume the following.*

1. *For signals with $\liminf_n \Lambda_n > 0$ and $\liminf_n \Xi_n > 0$, that $\sqrt{n}/q_n \rightarrow \infty$.*
2. *For signals with $\liminf_n \Lambda_n > 0$ and $\Xi_n \rightarrow 0$, that $\sqrt{n}\Xi_n/q_n \rightarrow \infty$.*
3. *For signals with $\Lambda_n \rightarrow 0$, that $\sqrt{n\Lambda_n}\Xi_n \geq (2 + \epsilon_n)\sqrt{-\log(\Lambda_n)}$, for some ϵ_n with $\epsilon_n\sqrt{-\log\Lambda_n}/q_n \rightarrow \infty$.*

Then, for such sequences $\vartheta_{\beta,n}$, the MQS selector for S is consistent, that is,

$$\mathbb{P}(\hat{S}(q_n) = S) \rightarrow 1.$$

Theorem 2.2 shows that for a sequence of signals $\vartheta_{\beta,n}$ the number of segments is estimated consistently as long as for the respective minimal scale Λ_n and minimal quantile jump Ξ_n it holds that

$$\sqrt{n\Lambda_n}\Xi_n > 2\sqrt{-\log(\Lambda_n)}. \quad (25)$$

Frick et al. (2014) showed that in the case of normal observations with piecewise constant mean, no method can consistently estimate the number of segments for a sequence of signals with minimal scale Λ_n and minimal jump height Δ_n whenever $\sqrt{n\Lambda_n}\Delta_n < \sqrt{-2\log(\Lambda_n)} + o(1)$. For Gaussian observations, the mean and the median coincide. Further, by Taylor expansion of the Gaussian cumulative distribution function, one obtains that $\Xi_n \in \mathcal{O}(\Delta_n)$. Consequently, possibly up to the constants, (25) cannot be improved in general.

Besides model selection consistency and confidence statements for all quantities, MQS also yields minimax optimal estimation rates for the location of segments (up to a log-factor) as the following theorem shows.

Theorem 2.3 (Estimation rates). *Consider the QSR-model with LHD-condition, $\hat{\vartheta} \in \mathcal{H}(q)$ as in (6), and Λ, Ξ as in (10). Then, for any $q > 0$ and sequence $\epsilon_n \searrow 0$*

$$\mathbb{P}\left(\max_{\tau \in J(\hat{\vartheta})} \min_{\hat{\tau} \in J(\hat{\vartheta}(q))} |\hat{\tau} - \tau| > \epsilon_n\right) \leq 4(S-1)e^{-n\epsilon_n\Xi^2} \left[e^{2\sqrt{n\epsilon_n}\Xi(q/\sqrt{2} + \sqrt{\log(2e/\epsilon_n)})} + 1 \right].$$

Note that for $\Lambda^{-1} = o(n/\log(n))$ and $q = o(\sqrt{\log(n)})$ a sufficient condition for the right hand side to vanish as $n \rightarrow \infty$ is $\epsilon_n \geq \log n/(\Xi^2 n)$, which, up to the log-term equals the minimax optimal sampling rate $1/n$ under a normal error assumption.

3. Implementation

The MQSE and its associated confidence bands are implemented using dynamic programming employing the double heap structure underlying the computation of quantiles as in (Astola and Campbell, 1989). The first part of the programming scheme is

analog to the one in (Frick et al., 2014). For sake of brevity, we only outline the major differences.

The local level α -tests in (17) can be inverted into $(1 - \alpha)$ -confidence statements for the underlying parameter θ_k as in (15). For $q > 0$ define $l(q)$ and $u(q)$ as the two unique solutions of

$$x \log\left(\frac{x}{\beta}\right) + (1 - x) \log\left(\frac{1 - x}{1 - \beta}\right) = q \quad (26)$$

such that $0 \leq l(q) < u(q) \leq 1$. Then, some straight forward calculations show that $T_n(Z, \vartheta) \leq q$ if and only if

$$\vartheta|_{[x_i, x_j]} \in \left[Z_{[\underline{m}_{i,j}]}^{i,j}, Z_{[\bar{m}_{i,j}+1]}^{i,j} \right] =: [\underline{b}_{ij}(q), \bar{b}_{ij}(q)], \forall i, j \text{ with } \vartheta|_{[x_i, x_j]} \text{ constant}, \quad (27)$$

with $\underline{m}_{i,j} = \max(1, \lceil (i - j + 1)l(\tilde{q}) \rceil)$, $\bar{m}_{i,j} = \min(n, \lfloor (i - j + 1)u(\tilde{q}) \rfloor)$ and $\tilde{q} = (q + P_{\ell,n}^2)/(2(j - i + 1))$. Note that $\underline{m}_{i,j} = \underline{m}_{1,j-i+1} =: \underline{m}_{j-i+1}$ and $\bar{m}_{i,j} = \bar{m}_{1,j-i+1} =: \bar{m}_{j-i+1}$ only depend on the length of interval $[x_i, x_j]$. Just as in (Frick et al., 2014), the computation of the multiscale estimator MQS is based on boxes on each interval $\{[\underline{b}_{ij}, \bar{b}_{ij}] : 1 \leq i \leq j \leq n\}$ in (27). However, whereas the boxes $\bar{b}_{ij}, \underline{b}_{ij}$ in (Frick et al., 2014) depend on the local sums of observations $\sum_{l=i}^j Z_l$, the respective boxes for MQS correspond to particular quantiles of the observations $\{Z_i, \dots, Z_j\}$. The dynamic program of (Frick et al., 2014) explores that the local sums and hence, boxes, of an interval $[i, j]$ can be updated in $\mathcal{O}(1)$ time from the boxes of intervals $[i - 1, j]$ and $[i - 1, j - 1]$, respectively. Thus, for efficient computation of the boxes $\bar{b}_{ij}, \underline{b}_{ij}$ of MQS one has to update the running quantiles $\bar{m}_1, \underline{m}_1, \dots, \bar{m}_n, \underline{m}_n$ efficiently. Here, we use double heap structures as in (Astola and Campbell, 1989) which update the running quantile in $\mathcal{O}(\log(n))$ time. Similar, the double heap structure allows to keep track of local runs of the transformed data, needed for sequential computation of the MQSE in $\mathcal{H}(q)$, recall (6) and Section 2.2.

In total, this increases the overall computation time by a log-factor, with worst case complexity of order $\mathcal{O}(n^2 \log(n))$. However, depending on the reconstructed signal, pruning steps and the use of smaller interval systems often lead to a computation time which is almost linear in the number of observations.

4. Simulations

In the following, we explore MQS in a simulation study. Thereby, the choice of the threshold parameter q is essential as it balances detection and overestimation of the number of segments and hence false positives. Thus, q can be seen as a tuning parameter of MQS. Via the one-to-one correspondence of a confidence level α and $q_n(\alpha)$ in (20), in the following, we choose $\alpha = 0.1$ and hence $q = q_n(0.1)$. In this way, the probability that MQS overestimates the number of segments does not exceed 10%. Such a choice depends on the application. However, we see a great advantage of our methodology, to rely only on this parameter, which has an immediate statistical meaning. For a more refined discussion on the choice of threshold parameter q and possible

	MQS	SMUCE	HSMUCE	WBS	R-FPOP	QS
Confidence statements	✓	✓	✓	✗	✗	✗
Consistency results	✓	✓	✓	✓	✓	✗
No distributional assumptions	✓	✗	✗	(✗)	✓	✓
All quantiles	✓	✗	✗	✗	(✗)	✓
Robust to outliers	✓	✗	✓	✗	✓	✓
Robust to heterogeneity	✓	✗	✓	✓	✗	✓
Computation time [s] (see caption)	0.65	0.01	0.02	0.07	0.01	38

Table 4.1: Summary table of the characteristics of MQS versus SMUCE (Frick et al., 2014), HSMUCE (Pein et al., 2017), WBS (Fryzlewicz, 2014), R-FPOP (Fearnhead and Rigaill, 2017) and, QS (Eilers et al., 2005). The computation time comparison is based on Model (28), with normal noise ($n = 1988$), mean as in Figure 4.1 and variance 0.04.

data driven model selection procedures, we refer to (Frick et al., 2014). For example, another possible parameter choice for q is via minimizing the right hand side of (12) together with Monte-Carlo simulations of M_n .

In the following, we consider five different competitors for MQS for which software is available online: SMUCE from (Frick et al., 2014), HSMUCE from (Pein et al., 2017), wild binary segmentation (WBS) from (Fryzlewicz, 2014), R-FPOP from (Fearnhead and Rigaill, 2017) and quantsmooth (QS) from (Eilers et al., 2005). SMUCE provides a multiscale methodology for normal observations with homogeneous variance. HSMUCE is also designed for normally distributed data, but is robust against changes in variance. WBS can be seen as a “greedy” procedure which successively adds changes based on a localized CUMSUM statistic. The theoretical results implicitly assume normally distributed observations with change in mean. R-FPOP is a penalized cost approach that uses the biweight loss, which is designed to be particularly robust to extreme outliers. It considers arbitrary changes in the underlying distribution, but cannot be tuned to search for changes in some specific quantile. In particular, it considers that observations in segments are i.i.d.. QS is a smoothing method which performs minimization of the asymmetric absolute deviation loss (recall Remark 2.4) together with L_1 penalization and hence, can compute arbitrary quantile curves. For all competitors, we choose tuning parameters as default in the available software. We summarize some features of these methods in Table 4.1. As measures of evaluation for the simulation study we use the number of estimated segments, the mean integrated squared error (MISE) $\sum_{i=1}^n (\hat{\vartheta}(x_i) - \vartheta_\beta(x_i))^2/n$, and the entropy-based V-measure introduced in (Rosenberg and Hirschberg, 2007). The latter takes values in $[0, 1]$ and measures whether given clusters include the correct data points of the correspond-

		Method	≤ 5	6	7	8	≥ 9	MISE	V-m.	≤ 5	6	7	8	≥ 9	MISE	V-m.
Normal $\sigma^2 = 0.04$	MQS(0.5)	0	0.9	99.1	0	0	2.37	9.28		0	11.2	87.6	0.2	0	2.47	9.32
	MQS(0.25)	81.9	18.1	0	0	0	6.73	8.63		83	17	0	0	0	6.77	8.65
	MQS(0.75)	0	0	99.9	0.1	0	4.44	9.02		0	0	99.8	0.2	0	4.74	9.06
	SMUCE	0	0	99.7	0.3	0	0.03	9.96		0	0	0	0	1	1.20	7.73
	HSMUCE	0	0	98.8	1.2	0	0.03	9.96	t (3 d.f.)	0	0	99.4	0.6	0	0.04	9.96
	R-FPOP	0	0	97.9	2	0.1	0.03	9.96	$\sigma^2 = 0.04$	0	0	95.4	4.3	0.3	0.03	9.97
	WBS	0	0	97.5	2.2	0.3	0.27	9.87		0	0	1.6	0.1	98.3	0.54	8.33
	QS(0.5)	0	0	0.1	0.2	99.7	4.39	3.54		0	0	0	0.1	99.9	4.29	3.55
	QS(0.25)	0.3	0.1	1.8	3.7	94.1	4.75	3.55		0	0.2	0.5	1.8	97.5	4.55	3.55
	QS(0.75)	0	0	0.1	0.4	99.5	1.77	3.54		0	0	0.3	99.7	1.55	3.54	
Cauchy	MQS(0.5)	0	17.4	82.5	0.1	0	2.63	9.34		0	0	99.7	0.3	0	2.43	9.33
	MQS(0.25)	87.7	12.2	0.1	0	0	6.97	8.67		80.1	19.9	0	0	0	6.72	8.74
	MQS(0.75)	0	0	99.9	0.1	0	5.25	9.08		0	0.2	99.8	0	0	4.58	8.93
	HSMUCE	0	0.4	99.6	0	0	0.23	9.81		0	0	88.1	11.3	0.6	9.31	9.91
	R-FPOP	0	0	91.5	6.3	2.2	0.03	9.98	χ^2_3	0	0	85	8.9	6.1	0.09	9.93
	WBS	0	0	0	0	100	5.57	6.88	$\sigma^2 = 0.04$	0	0	26	0.6	73.4	0.32	9.31
	QS(0.5)	0	0	0	0.1	99.9	4.21	3.55		0	0.1	0	0.1	99.8	4.40	3.55
	QS(0.25)	0	0.1	0.1	1.1	98.7	4.30	3.55		0	0.7	1.6	2.1	95.6	4.47	3.54
	QS(0.75)	0	0	0	0.1	99.9	1.22	3.54		0	0	0.2	0.4	99.4	2.24	3.54

Table 4.2: Frequencies of estimated number of segments in [%], MISE ($\times 100$), and V-measure ($\times 10$) for data as in Figure 4.1. Here, the true number of segments equals 7. The proposed MQS estimator is compared with SMUCE (Frick et al., 2014), HSMUCE (Pein et al., 2017), WBS (Fryzlewicz, 2014), R-FPOP (Fearnhead and Rigaill, 2017) and QS (Eilers et al., 2005).

ing class. Larger values indicate higher accuracy with 1 corresponding to a perfect segmentation. All results were obtained from 1,000 Monte Carlo runs.

4.1. Additive error

First, we consider an additive model with i.i.d. error terms, that is,

$$Z_i = \vartheta(x_i) + \varepsilon_i \quad \text{for } i = 1, \dots, n \quad (28)$$

with $\vartheta \in \Sigma$ and $\varepsilon_1, \dots, \varepsilon_n$ i.i.d. according to some distribution. For observations as in (28) in the QSR-model the quantile functions ϑ_β are shifted versions of ϑ , namely, $\vartheta_\beta = \vartheta + \theta_\beta$, where θ_β is the β -quantile of ε_1 . In particular, for any quantile $\beta \in (0, 1)$, ϑ_β has the same number and locations of segments. Here, we consider ϑ as in Figure 4.1 (top row), which has 7 segments and $n = 1,988$. For the error terms ε_i we consider normal distribution $\varepsilon_i \sim \mathcal{N}(0, \sigma^2)$, t -distribution with 3 degrees of freedom $\varepsilon_i \sim t_3\sigma/\sqrt{3}$ and variance σ^2 , rescaled Cauchy distribution (heavy tails) $\varepsilon_i \sim 0.02 \text{Cauchy}(0, 1)$, and rescaled chi-square distribution (skewed) with 3 degrees of freedom and median 0, that is, $\varepsilon_i \sim (\chi^2_3 - \beta_{0.5}(\chi^2_3))\sigma/\sqrt{6}$ with variance σ^2 , with $\sigma^2 = 0.04$ and $\beta_{0.5}(\chi^2_3)$ the median of the distribution χ^2_3 . (see Figure 4.1).

The results for MQS(β), $\beta = 0.25, 0.5, 0.75$ are shown in Table 4.2. Note that, in general, the MQS selector of S for $\beta = 0.5, 0.75$ seems to have a higher detection power as for $\beta = 0.25$ in this example. This is due to the fact that the test signal ϑ in Figure 4.1 (top row) has 4 jumps upwards but just 2 jumps downwards. It is easy to check that jumps upwards have a stronger influence on higher (overall) empirical quantiles. MQS is a reasonable estimator in the four scenarios presented in this section. It is robust against outliers, as well as to skewness of the distributions. For normally

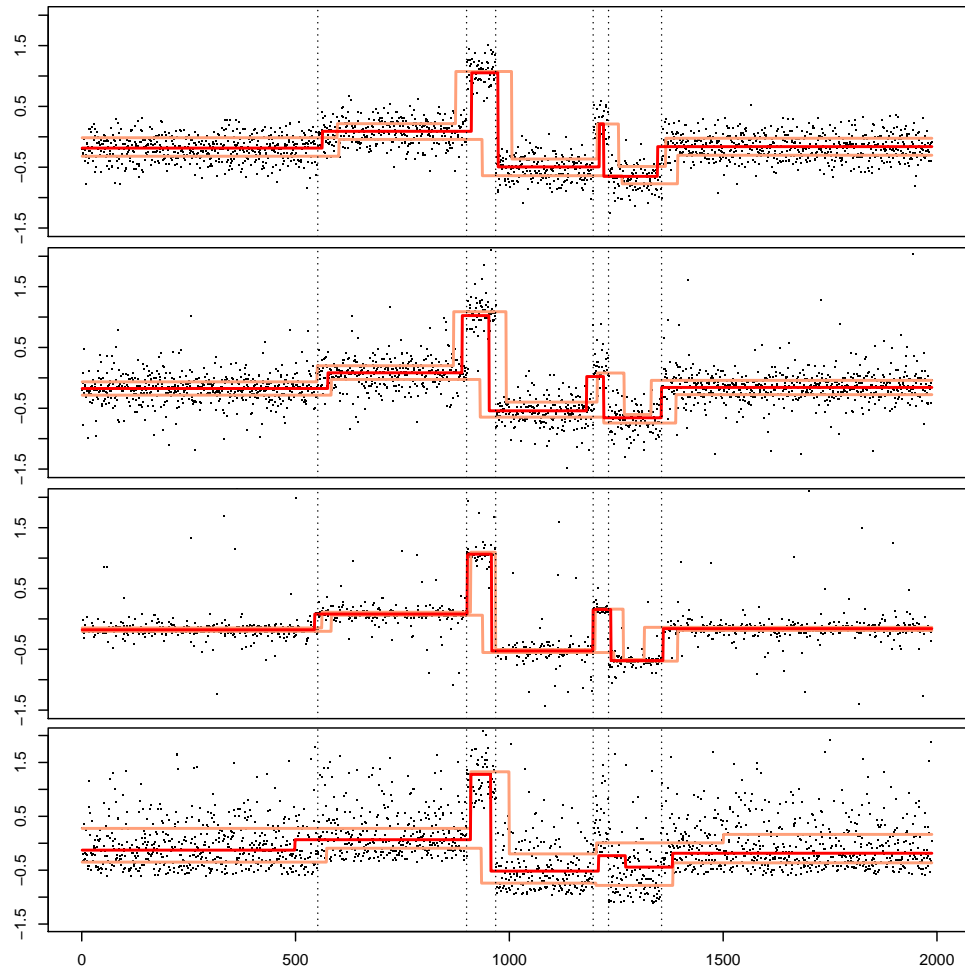


Figure 4.1: Realizations as in (28) (black dots) for $n = 1,988$ and different error terms. The true underlying segment changes are shown as dotted vertical lines. The corresponding MQS multiscale box plot with threshold parameter $q = q_n(0.1)$ is shown in red (median) and light red lines (0.25- and 0.75 quantiles). From top to bottom: normally distributed with variance $\sigma^2 = 0.04$, t distributed with 3 degrees of freedom and variance $\sigma^2 = 0.04$, Cauchy distributed, χ^2 distributed with 3 degrees of freedom and variance $\sigma^2 = 0.04$.

	Method	≤ 3	4	5	6	≥ 7	MISE	V-m.		≤ 3	4	5	6	≥ 7	MISE	V-m.
Normal	MQS(0.5)	17.3	82	0.7	0	0	2.42	8.69		0	99.3	0.7	0	0	1.94	9.02
	MQS(0.25)	0.5	64.8	34.3	0.4	0	4.84	7.27		3.5	58.8	32.3	5.4	0	3.99	7.21
	MQS(0.75)	0	0.4	57.4	42.2	0	5.85	7.48		0	2	74.6	23.4	0	4.47	7.49
	SMUCE	0.1	34.9	36.3	19	9.7	0.46	8.72		0	0	0	0	100	18.52	5.63
	R-FPOP	0	65.1	10.5	13	11.4	0.61	9.36	t (3 d.f.)	0	78.8	7.8	9.1	4.3	0.25	9.67
	WBS	0.9	92.5	1.7	4.3	0.6	0.45	9.67		0	0	0.1	0.5	99.4	4.33	6.64
	HSMUCE	26.4	72.4	1.2	0	0	0.51	9.64		12.4	86.5	1.1	0	0	0.38	9.72
	QS(0.5)	0	0.3	0.6	2.7	96.4	1.78	2.56		0	0.2	0.9	2.5	96.4	0.78	2.56
	QS(0.25)	1	4.6	11.7	19.1	63.6	6.38	3.65		2.6	10.8	16.6	22.3	47.7	4.05	3.65
	QS(0.75)	0	0	0	0	100	2.91	3.65		0	0	0	0	100	2.18	3.65

Table 4.3: Frequencies of estimated number of segments (in percentage), MISE($\times 100$) and V-measure($\times 10$) for changes of variance, as well as of mean for data as in Figure 4.2. The true number of segments for the median is 4 and for the other quantiles 6.

distributed data, both SMUCE and WBS, slightly outperform MQS, in particular in terms of MISE and segmentation accuracy. However, for heavy tailed distributions as well as for skewed distributions SMUCE and WBS fail completely, while MQS retains a very high segmentation accuracy. R-FPOP performs comparably to MQS in all four scenarios of this setting, slightly outperforming MQS in terms of MISE. HSMUCE also performs comparably to MQS, except in the χ^2_3 case where MQS performs better. QS performs comparably to MQS in terms of MISE, however, it highly overestimates the number of segments and performs worse in terms of estimation accuracy and computational speed.

4.2. Changes in variance

The QSR-model further allows for changes in variance or other characteristics which are independent of changes in the respective β quantile ϑ_β . Here, we consider changes in variance for normally and t distributed (with 3 degrees of freedom) observations and $n = 2,000$. In Figure 4.2 (top row) the underlying median (mean) (solid line) and variance (dashed line) functions are displayed. The second and third row show the true 0.25, 0.5, and 0.75 quantile functions (black lines) and the MQS box plot (red lines). Note that in this example, the 0.5 quantile has 4 segments and the 0.25 and 0.75 quantiles have 6 segments. Simulation results are shown in Table 4.3. The MQSE appears to be very robust against changes in variance within a segment even for heavy tailed distributions. It estimates the correct number of change points with high probability. At the same time, the MQSE for the 0.25 and 0.75 quantiles depict changes in variance. Similar, WBS is robust to changes in variance and slightly outperforms MQSE for normally distributed data. HSMUCE performs comparably to the MQSE in this setting. However, just as SMUCE, HSMUCE is restricted to change in mean and is not robust to outliers or skewness. In the heavy tailed case, WBS highly overestimates the number of change points, in contrast to MQS. R-FPOP performs significantly worse than MQS in this setting, as it is not robust to changes in variance. This is because R-FPOP is designed to detect arbitrary distributional changes. Just as in the previous section, QS highly overestimates the number of segments.

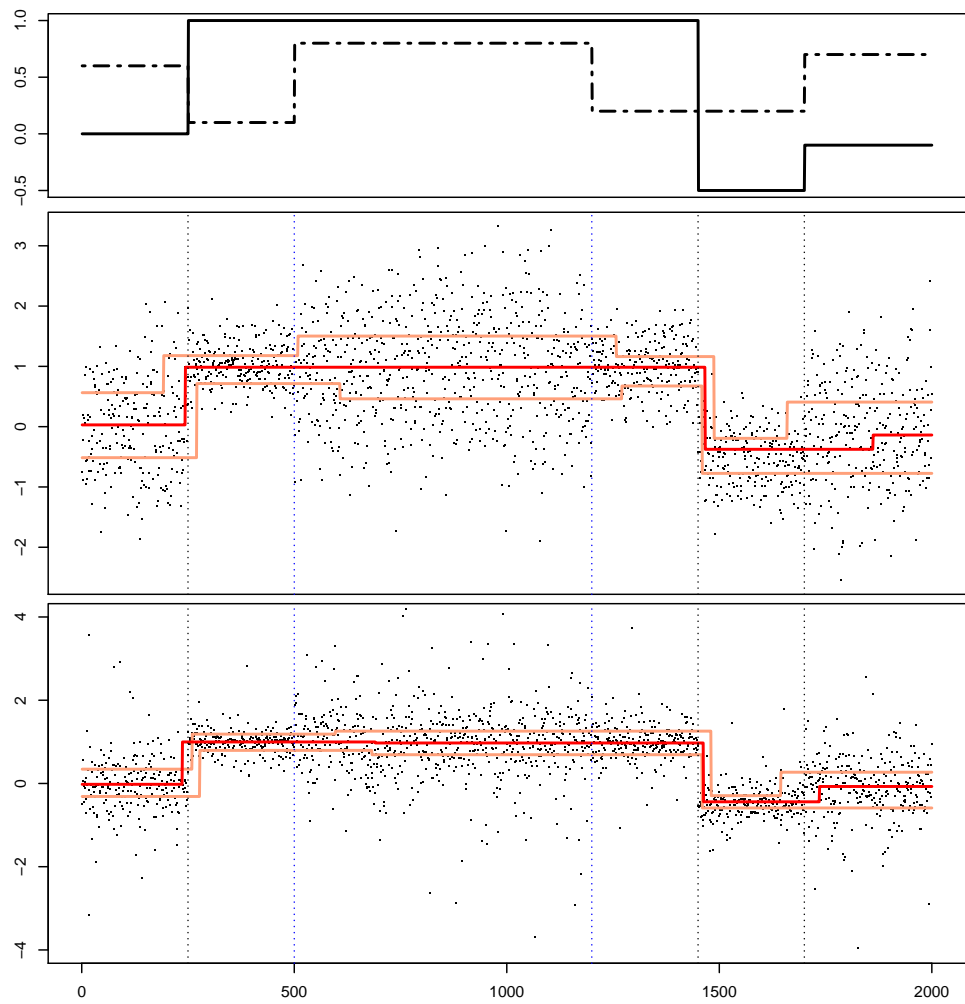


Figure 4.2: Top row: underlying mean (solid line) and variance (dashed line) functions. Subsequent rows: normally and t distributed (from top to bottom) observations (black dots) with $n = 2,000$ and mean and variance as in top row, together with the MQS box plot (red lines). The true location of segment changes is shown as a vertical dotted lines, the blue dotted lines correspond to changes only in the 0.25- and 0.75-quantiles.

4.3. Confidence statements

MQS also provides confidence statements for the number of segments, the change point locations, and finally the underlying segment function itself (see Remark 2.5). In this section, we investigate the behavior of such confidence statements in the additive error models as considered in Figure 4.1, with $n = 2485$. Simulation results are shown in Table 4.4. An example for $\beta = 0.5, 0.25, 0.75$ with data as in Example 1.1 is shown in Figure 1.1.

As demonstrated in Section 4.1, the number of segments is estimated correctly with high probability for $\beta = 0.5, 0.75$ and slightly underestimated for $\beta = 0.25$. Our method gives the theoretical guarantee that $P(\hat{S} \leq S) \geq 1 - \alpha$ (see (8)). In Table 4.4, we give the frequency of $\hat{S} \leq S$ for $n = 2485$. For all considered examples, (8) is fulfilled for a much larger level than required. Moreover, given that the number of segments is estimated correctly, we construct simultaneous confidence intervals for the true change point locations (see blue intervals in Figure 1.1). In Table 4.4 column "CI cov." (short for Confidence Interval coverage), we give the frequency that all the change points τ_s were inside the respective confidence intervals (given that $\hat{S} = S$), for $n = 2485$. We find that with very high probability, all the change points are covered by the confidence intervals. We also provide confidence bands that cover the true function with probability at least $1 - \alpha$ (see Remark 2.5), given that the number of change points is estimated correctly (see gray area in Figure 1.1). In Table 4.4 column "CB cov." (short for Confidence Band coverage), we give the frequency that the true function ϑ was fully inside the confidence band (given that $\hat{S} = S$), for $n = 2485$. Here, we see that the nominal level is kept, but the confidence bands are, in general, too conservative. Figure 1.1 shows that the confidence intervals and bands are sharper around the median than around the 0.25– and 0.75–quantiles, with the 0.25–quantile having the largest intervals and bands. This reflects the fact that quantiles closer to 0 or 1 are harder to estimate, in general.

	β	$1 - \alpha$	$\mathbb{P}(\hat{S} \leq S)$	CI cov.	CB cov.		$\mathbb{P}(\hat{S} \leq S)$	CI cov.	CB cov.
Normal $\sigma^2 = 0.04$	0.5	0.99	1.000	1.000	0.998	t (3 d.f.) $\sigma^2 = 0.04$	1.000	1.000	0.996
		0.95	1.000	1.000	0.977		1.000	1.000	0.974
		0.90	0.997	1.000	0.936		0.998	1.000	0.947
	0.25	0.99	1.000	1.000	1.000		1.000	1.000	1.000
		0.95	1.000	1.000	0.994		1.000	1.000	0.996
		0.90	0.999	1.000	0.951		0.998	1.000	0.948
	0.75	0.99	1.000	1.000	0.998		1.000	1.000	0.998
		0.95	0.999	1.000	0.962		0.999	1.000	0.972
		0.90	0.998	1.000	0.953		0.998	0.999	0.954
Cauchy	0.5	0.99	1.000	1.000	0.998	χ^2_3 $\sigma^2 = 0.04$	1.000	1.000	0.993
		0.95	0.999	1.000	0.965		0.999	1.000	0.966
		0.90	0.995	0.998	0.928		1.000	0.998	0.936
	0.25	0.99	1.000	1.000	1.000		1.000	1.000	1.000
		0.95	1.000	1.000	0.997		1.000	1.000	0.994
		0.90	1.000	1.000	0.943		0.998	1.000	0.955
	0.75	0.99	1.000	1.000	0.995		1.000	1.000	0.992
		0.95	1.000	1.000	0.971		1.000	1.000	0.977
		0.90	0.999	0.999	0.932		0.998	0.999	0.952

Table 4.4: Probability of estimating correctly the number of segments, frequency of confidence interval coverage of the true c.p.’s (CI cov.), and frequency of confidence band coverage of the true function (CB cov.), for data as in Figure 4.1 with different levels α and $n = 2485$.

5. Real data examples

5.1. Copy Number Aberrations

Copy Number Aberrations (CNA’s) are sections of DNA in the genome of cancer cells that are either multiplied or deleted, relative to the state present in normal tissue. CNA’s are important factors of tumor progression, through the deletion of tumor suppressing genes and the multiplication of genes involved for example in cell division. The number of copies of DNA sections, depending on chromosomal loci, corresponds to a segment function, where a segment corresponds to a different copy number. A common measurement technique is via whole genome sequencing (WGS). Thereby, the tumor DNA is fragmented into several pieces. Then the single pieces are sequenced using short “reads”, and finally these reads are aligned to a reference genome by a computer. Statistical modeling of WGS data is particularly difficult as random variations and systematic biases, such as mappability and CG bias, lead to violations of parametric model assumptions, such as normal or Poisson, see e.g. (Liu et al., 2013). Quantile segmentation with MQS does not require any such specific model assumptions and hence, is particularly suited for this setting.

Figure 1.4 shows (pre-processed¹) WGS data of cell line LS411 from colorectal cancer. Sequencing was performed by Complete Genomics in collaboration with the Well-

¹Sequencing produces spatial artifacts in the data and waviness, which can be pre-process using standard procedures of smoothing filter, baseline correction and binning, see e.g., (Behr, 2018) for details.

come Trust Centre for Human Genetics at the University of Oxford. For this particular data set, it is known that the underlying CNA's only take values in the natural numbers. This is because it was collected under special conditions, where cells come from a single homogeneous tumor-clone, see (Behr, 2018) for more details. This allows certain validation of the estimated segments, something which is not feasible for most real patient tumors.

The top row of Figure 1.4 shows the MQS multiscale box plot (the estimated 0.25, 0.5, and 0.75 quantiles) at confidence level $1 - \alpha = 0.99$. MQSE recovers most of the signal structure correctly. In particular, MQSE is way more robust than SMUCE (Frick et al., 2014) (second row in Figure 1.4), WBS (Fryzlewicz, 2014) (third row in Figure 1.4), and R-FPOP (Fearnhead and Rigaill, 2017) (fourth row in Figure 1.4). SMUCE, WBS and R-FPOP introduce many artificial small changes, which cannot be present in the underlying signal as, in this particular example, it is known to only take integer values. HSMUCE (Pein et al., 2017) (fifth row in Figure 1.4) is more robust, but still adds artificial changes. The sixth row of Figure 1.4 shows the estimated 0.25, 0.5, and 0.75 quantiles of QS (Eilers et al., 2005). Similar to MQS, it correctly recovers most of the signal structure, but it misses some underlying changes, see, in particular, the last change at data point 7148. Moreover, QS has a much higher running time compared to MQS: while MQS took 31 seconds to run each quantile for this data set, QS took 54 minutes.

5.2. Ion channel data

Ion channels are pore-forming proteins that allow ions to pass through a cell membrane. They are vital for several processes like excitation of neurons and muscle cells. The pores of an ion channel can open and close, a process called *gating*, often as a result of external stimuli. Therefore, the amount of ions that can pass through a channel is not constant in time, due to gating or the passage of larger proteins (Chung et al., 2007). A major tool for a quantitative analysis of the gating dynamics is the *patch clamp* technique, which allows to measure the conductance of a single ion channel in time (Sakmann and Neher, 1995). Roughly speaking, this kind of data is obtained by inserting a single ion channel in an (often artificial) membrane surrounded by an electrolyte with an electrode to measure the current while constant voltage is applied. These recordings can be modeled as a segment function disturbed by an error, see e.g. (Pein et al., 2017; Gnanasambandam et al., 2017).

The particular data set considered in Figure 5.1 comes from a single channel of the bacterial porin PorB from the Steinam lab (Institute of Organic and Biomolecular Chemistry, University of Göttingen). PorB is the outer membrane porin from *Neisseria meningitidis*, a pathogenic bacteria well known for being the agent of epidemic meningitis (Virji, 2009). The measurement protocol incorporates a lowpass filter which leads to local dependencies of the error terms, see (Pein et al., 2017). To remove these dependencies, which violate modeling assumptions of the QSR-model, we subsampled every 11th observation.

The MQS multiscale box plot is shown in the top row of Figure 5.1. A common feature of ion channel data, called open channel noise, is that the noise variance in

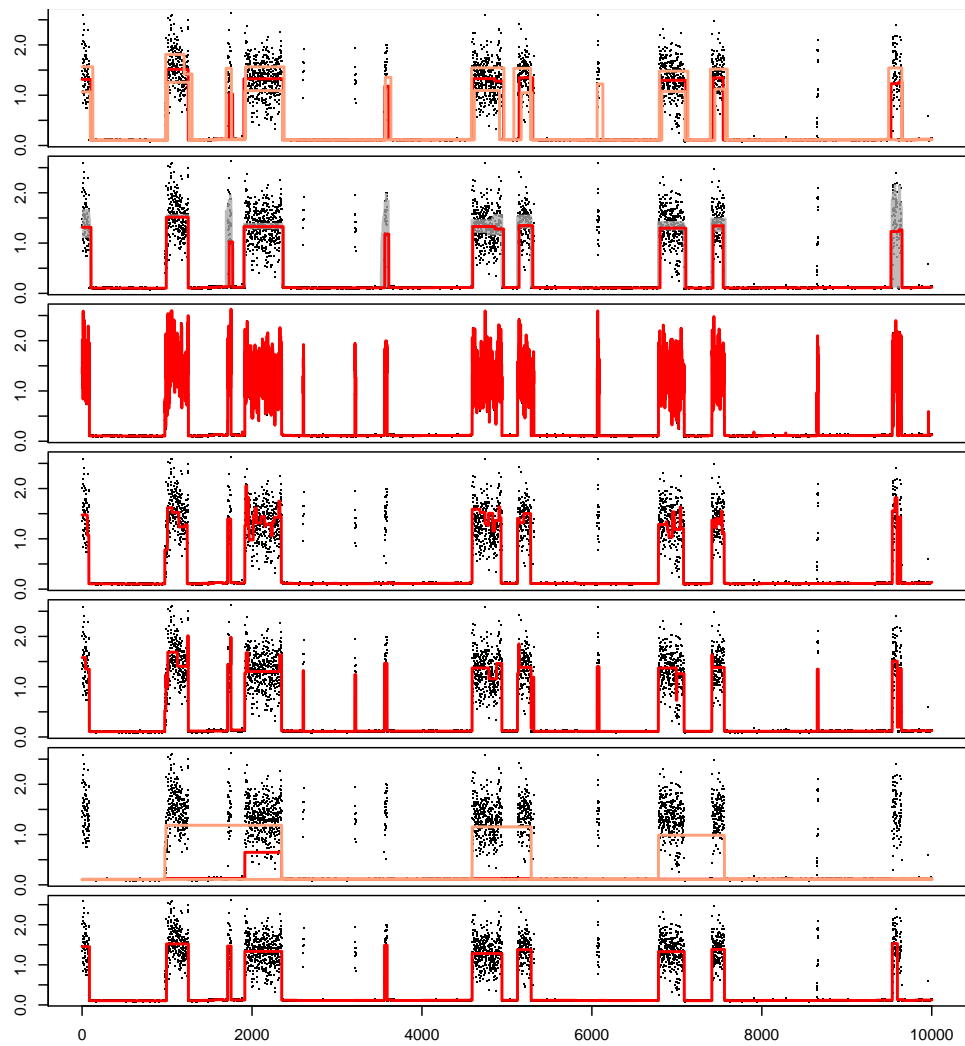


Figure 5.1: Ion channel data (black dots) from a single channel of the bacterial porin PorB from the Steinam lab (Institute of Organic and Biomolecular Chemistry, University of Göttingen). From top to bottom: MQS multiscale box plot with $\alpha = 0.1$, MQSE for the median with confidence bands, SMUCE (Frick et al., 2014), RFPOP (Fearnhead and Rigaill, 2017), WBS (Fryzlewicz, 2014), QS (Eilers et al., 2005) (together with 0.25- and 0.75-quantiles) and HSMUCE (Pein et al., 2017).

open states is often much higher than in closed states, see (Sakmann and Neher, 1995, Section 3.4.4). MQS is very robust against this heterogeneity while at the same time reliably detects most of gating events. SMUCE (Frick et al., 2014), R-FPOP (Fearnhead and Rigaill, 2017), and WBS (Fryzlewicz, 2014) (second to fourth rows in Figure 5.1) introduce a lot of artificial changes, because of the change in variance due to the open channel noise. QS (Eilers et al., 2005) (fifth row in Figure 5.1) misses most of the structural segment changes in all quantiles. The bottom row of Figure 5.1 shows the reconstruction with HSMUCE (Pein et al., 2017), which assumes normal observations with possible changes in variance. Although HSMUCE is particularly tailored to this application, its reconstruction does not seem to be superior to MQS. Moreover, in contrast to HSMUCE, MQS explicitly quantifies the change in variance via the inter-quantile distance in the multiscale box plot.

Acknowledgments

The authors acknowledge support of DFG-RTG 2088 and DFG-SFB 803 Z02. Helpful comments from Chris Holmes, Housen Li, and Florian Pein are gratefully acknowledged.

Appendix A Proofs of Section 2

The proofs of this section follow the spirit of the proofs on (Frick et al., 2014). However, there are important differences due to the discrete nature of the transformation (3) and the convergence rates of the empirical quantiles. Before we prove the main results of Section 2, we give a couple of auxiliary results.

To this end, let W_1, W_2, \dots, W_n be i.i.d. Bernoulli distributed random variables with mean β and

$$h_k(x) = x \log \frac{x}{k\beta} + (k-x) \log \frac{k-x}{k(1-\beta)}.$$

For fixed n define the random variables

$$\xi(i, j) = \sqrt{2h_{j-i+1} \left(\sum_{k=i}^j W_k \right)} - \sqrt{2 \log \left(\frac{e n}{j-i+1} \right)}.$$

Theorem A.1. *Let $k \in \mathbb{N}$ with $k \geq 1$ and $q_n(\alpha)$ as in (20). Then*

$$\mathbb{P} \left(\min_{1 \leq s \leq k} \xi(i_s, j_s) > q_n(\alpha) \text{ for some } 1 \leq i_1 \leq j_1 < \dots < i_k \leq j_k \leq n \right) \leq \alpha^k.$$

Proof. Define the stopping times

$$\begin{aligned} \zeta_0(q) &= 1, \\ \zeta_k(q) &= \min \left\{ j > 1 : \max_{\zeta_{k-1}(q) < i \leq j} \xi(i, j) > q \right\}. \end{aligned}$$

Note that

$$\begin{aligned}
\zeta_{k+1}(q) - \zeta_k(q) + 1 &= \min \left\{ j - \zeta_k(q) > 0 : \max_{\zeta_k(q) < i \leq j} \xi(i, j) > q \right\} \\
&= \min \left\{ j > 1 : \max_{\zeta_k(q) < i \leq j + \zeta_k(q) - 1} \xi(i, j + \zeta_k(q) - 1) > q \right\} \\
&= \min \left\{ j > 1 : \max_{1 < i \leq j} \sqrt{2h_{j-i+1} \left(\sum_{r=i}^j W_{r+\zeta_k(q)-1} \right)} - \sqrt{2 \log \left(\frac{e n}{j-i+1} \right)} > q \right\}.
\end{aligned}$$

Consider the Markov process $(\sum_{i=1}^n W_i)_{n \in \mathbb{N}}$. By the strong Markov property, for any stopping time τ the process $(\sum_{i=1}^n W_{i+\tau})$ is independent of W_1, \dots, W_τ conditioned on $\tau < \infty$. Note also that $(\sum_{i=1}^n W_{i+\tau})$ is identically distributed for all stopping times τ , because it is the sum of n i.i.d. random variables. This implies that

$$\zeta_1(q), \zeta_2(q) - \zeta_1(q) + 1, \zeta_3(q) - \zeta_2(q) + 1, \zeta_4(q) - \zeta_3(q) + 1, \dots$$

are independent and identically distributed. Therefore, for any $k \geq 1$ and $x > 0$ it follows that

$$\mathbb{P}(\zeta_k(q) - 1 \leq x) = \mathbb{P} \left(\sum_{l=1}^k \zeta_l(q) - \zeta_{l-1}(q) \leq x \right) \leq \mathbb{P}(\zeta_1(q) - 1 \leq x)^k.$$

By definition $\zeta_1(q) \leq n$ implies that $M_n > q$, for M_n as in (7). Therefore, it follows from (20) that

$$\mathbb{P}(\zeta_1(q_n(\alpha)) \leq n) \leq \mathbb{P}(M_n > q_n(\alpha)) \leq \alpha.$$

□

For the following two theorems let Z_1, \dots, Z_n be i.i.d. random variables with distribution function F and, for given $\beta \in (0, 1)$, define the population and empirical quantiles

$$\begin{aligned}
\theta_\beta &:= F^{-1}(\beta) := \inf\{x \in \mathbb{R} : F(x) \geq \beta\}, \\
\hat{\theta}_\beta &:= \inf\{x \in \mathbb{R} : \sum_{i=1}^n \mathbb{1}_{Z_i \leq x} \geq n\beta\}.
\end{aligned} \tag{29}$$

Theorem A.2. *Let $\xi_{F,\beta}$ be as in Definition 1.1. Then for any $\delta > 0$*

$$\begin{aligned}
\mathbb{P}(\hat{\theta}_\beta - \theta_\beta > \delta) &\leq 2 \exp(-2n \xi_{F,\beta}(\delta)^2), \\
\mathbb{P}(\theta_\beta - \hat{\theta}_\beta > \delta) &\leq 2 \exp(-2n \xi_{F,\beta}(-\delta)^2).
\end{aligned}$$

Proof. Note that for any distribution function it holds that $F(x) \geq y$ if and only if $x \geq F^{-1}(y)$. This implies that $F(x) < y$ if and only if $x < F^{-1}(y)$. Therefore

$$\begin{aligned}\mathbb{P}(\hat{\theta}_\beta - \theta_\beta > \delta) &= \mathbb{P}(\mathbb{F}_n^{-1}(\beta) > \theta_\beta + \delta) \\ &= \mathbb{P}(\beta > \mathbb{F}_n(\theta_\beta + \delta)) \\ &= \mathbb{P}(F(\theta_\beta + \delta) - \mathbb{F}_n(\theta_\beta + \delta) > F(\theta_\beta + \delta) - \beta) \\ &\leq 2 \exp(-2n \xi_{F,\beta}(\delta)^2)\end{aligned}$$

where the last inequality follows from the Dvoretzky-Kiefer-Wolfowitz inequality, see e.g. (Massart, 1990). The other inequality follows analog. \square

Theorem A.3. *Let T_1^n be as in (16) and W as in (3). Then, for any $\delta, \epsilon > 0$*

$$\mathbb{P}(T_1^n(W(Z, \theta_\beta + \delta), \beta) \leq \epsilon) \leq 2 \exp\left\{-\left(\sqrt{2n} \xi_{F,\beta}(\delta) - \sqrt{\epsilon}\right)_+^2\right\}.$$

Proof. For any $p, q \in (0, 1)$, Pinsker's inequality, see e.g. (Tsybakov, 2009, Lemma 2.5), implies

$$p \log \frac{p}{q} + (1-p) \log \frac{1-p}{1-q} \geq 2(p-q)^2. \quad (30)$$

Recall that W_1, \dots, W_n are i.i.d. Bernoulli distributed with mean $F(\theta_\beta + \delta)$, for $W = W(Z, \theta_\beta + \delta)$. Define $\bar{W} = n^{-1} \sum_{i=1}^n W_i$ and assume that $\xi_{F,\beta}(\delta) > \sqrt{\epsilon/2n}$ (otherwise the assertion follows trivially). Then (30) implies

$$\begin{aligned}\mathbb{P}(T_1^n(W(Z, \theta_\beta + \delta), \beta) \leq \epsilon) &\leq \mathbb{P}\left(2(\bar{W} - \beta)^2 \leq \epsilon/n\right) \\ &= \mathbb{P}\left(|\bar{W} - \beta| \leq \sqrt{\epsilon/2n}\right) \\ &= \mathbb{P}\left(|\bar{W} - F(\theta_\beta + \delta) - \beta + F(\theta_\beta + \delta)| \leq \sqrt{\epsilon/2n}\right) \\ &\leq \mathbb{P}\left(|\beta - F(\theta_\beta + \delta)| - |\bar{W} - F(\theta_\beta + \delta)| \leq \sqrt{\epsilon/2n}\right) \\ &= \mathbb{P}\left(|\bar{W} - F(\theta_\beta + \delta)| \geq \xi_{F,\beta}(\delta) - \sqrt{\epsilon/2n}\right) \\ &\leq 2 \exp\left(-2n \left(\xi_{F,\beta}(\delta) - \sqrt{\epsilon/2n}\right)^2\right) \\ &= 2 \exp\left\{-\left(\sqrt{2n} \xi_{F,\beta}(\delta) - \sqrt{\epsilon}\right)_+^2\right\}\end{aligned}$$

where the last inequality follows from Hoeffding's inequality. \square

Now we are ready to prove the main results of Section 2.

Proof of Theorem 1.1. Let $J(\vartheta)$ denote the set of change points of ϑ . First, note that

$$\begin{aligned} \mathbb{P}(\hat{S}_{n,\alpha} > S + 2s) &= \mathbb{P}(T_n(Z, \hat{\vartheta}) > q_n(\alpha), \forall \hat{\vartheta} \in \Sigma \text{ with } \#J(\hat{\vartheta}) \leq S + 2s - 1) \\ &\leq \mathbb{P}(T_n(Z, \hat{\vartheta}) > q_n(\alpha), \forall \hat{\vartheta} \in \Sigma \text{ with } J(\vartheta) \subseteq J(\hat{\vartheta}), \#J(\hat{\vartheta}) \leq S + 2s - 1) \\ &\leq \mathbb{P}(T_n(Z - \vartheta, \hat{\vartheta} - \vartheta) > q_n(\alpha), \forall \hat{\vartheta} \in \Sigma \text{ with } \#J(\hat{\vartheta} - \vartheta) \leq 2s) \\ &\leq \mathbb{P}(T_n(\tilde{Z}) > q_n(\alpha), \forall \tilde{\vartheta} \in \Sigma \text{ with } \#J(\tilde{\vartheta}) \leq 2s) = \mathbb{P}(\tilde{S}_{n,\alpha} > 1 + 2s), \end{aligned}$$

with $\tilde{Z} = Z - \vartheta$ and $\tilde{S}_{n,\alpha}$ as in (5) with Z replaced by \tilde{Z} . Thus, we can assume w.l.o.g. that $\vartheta \equiv \theta_0$ and $S = 1$.

Observe that $\hat{S}_{n,\alpha} \geq 2s + 2$ implies that the multiscale constraint for the true regression function ϑ is violated on at least $s + 1$ disjoint intervals $[i_1/n, j_1/n], \dots, [i_{s+1}/n, j_{s+1}/n] \subseteq [0, 1]$, that is

$$\sqrt{2T_{i_k}^{j_k}(W(Z, \vartheta_\beta), \beta)} - \sqrt{2 \log \left(\frac{e n}{j_k - i_k + 1} \right)} > q(\alpha) \quad \text{for all } 1 \leq k \leq s + 1$$

and it follows from Theorem A.1 that

$$\begin{aligned} &\mathbb{P} \left(\exists (1 \leq i_1 \leq j_1 \leq \dots \leq j_{s+1} \leq n) : \min_{1 \leq k \leq s+1} \sqrt{2T_{i_k}^{j_k}(W, \beta)} \right. \\ &\quad \left. - \sqrt{2 \log \left(\frac{e n}{j_k - i_k + 1} \right)} \geq q_n(\alpha) \right) \\ &\leq \mathbb{P} \left(\exists (1 \leq i_1 \leq j_1 \leq \dots \leq i_{s+1} \leq j_{s+1} \leq n) : \min_{1 \leq k \leq s+1} \xi(i_k, j_k) \geq q(\alpha) \right) \\ &\leq \alpha^{s+1}. \end{aligned}$$

□

Proof of Theorem 2.1. Define for $s = 1, \dots, S - 1$ the intervals

$$I_s = (\tau_s - \lambda_s/2, \tau_s + \lambda_s/2].$$

Note that these intervals are pairwise disjoint because $\lambda_s \leq \min\{\tau_s - \tau_{s-1}, \tau_{s+1} - \tau_s\}$.

Let $\theta_s^+ = \max\{\theta_s, \theta_{s+1}\}$ and $\theta_s^- = \min\{\theta_s, \theta_{s+1}\}$ and split the interval I_s accordingly, i.e.

$$I_s^+ = \{t \in I_s : \vartheta(t) = \theta_s^+\} \quad \text{and} \quad I_s^- = \{t \in I_s : \vartheta(t) = \theta_s^-\}.$$

We are interested in the event that a function exists which is constant on I_s and fulfills the multiscale constraints in both I_s^- and I_s^+ , i.e.

$$\begin{aligned} \Omega_s = \left\{ \exists \hat{\theta} \in \mathbb{R} : \sqrt{2T_{I_s^+}(W(Z, \hat{\theta}), \beta)} - \sqrt{2 \log \frac{e n}{\#I_s^+}} \leq q \text{ and} \right. \\ \left. \sqrt{2T_{I_s^-}(W(Z, \hat{\theta}), \beta)} - \sqrt{2 \log \frac{e n}{\#I_s^-}} \leq q \right\}. \quad (31) \end{aligned}$$

Observe that either $\hat{\theta} \leq \theta_s^+ - \delta_s/2$ or $\hat{\theta} \geq \theta_s^- + \delta_s/2$ and define

$$\Omega_s^+ = \left\{ \exists \hat{\theta} \leq \theta_s^+ - \delta_s/2 : \sqrt{2T_{I_s^+}(W(Z, \hat{\theta}), \beta)} - \sqrt{2 \log \frac{e n}{\#I_s^+}} \leq q \right\},$$

$$\Omega_s^- = \left\{ \exists \hat{\theta} \geq \theta_s^- + \delta_s/2 : \sqrt{2T_{I_s^-}(W(Z, \hat{\theta}), \beta)} - \sqrt{2 \log \frac{e n}{\#I_s^-}} \leq q \right\}.$$

Due to the independence of Ω_s^+ and Ω_s^- and the fact that $\Omega_s \subseteq \Omega_s^+ \cup \Omega_s^-$, we get that

$$\mathbb{P}(\Omega_s) \leq 1 - (1 - \mathbb{P}(\Omega_s^+))(1 - \mathbb{P}(\Omega_s^-)).$$

Next, we prove an upper bound for $\mathbb{P}(\Omega_s^-)$; a bound for $\mathbb{P}(\Omega_s^+)$ follows from symmetry.

Let F denote the distribution function of the random variables in I_s^- , then $F^{-1}(\beta) = \theta_s^-$. Let

$$\zeta_{I_s^-} := \inf \left\{ x \in \mathbb{R} : \sum_{i \in I_s^-} \mathbb{1}_{Z_i \leq x} \geq |I_s^-| \beta \right\} \quad (32)$$

be the empirical quantile of the observations on the interval I_s^- . Thus, for all $\hat{\theta} \geq \theta_s^- + \delta_s/2$, if $\zeta_{I_s^-} \leq \theta_s^- + \delta_s/2$, we get that

$$\beta \leq \overline{W}(Z, \zeta_{I_s^-}) \leq \overline{W}(Z, \theta_s^- + \delta_s/2) \leq \overline{W}(Z, \hat{\theta}). \quad (33)$$

Moreover, the function

$$f : x \mapsto |I_s^-| \left(x \log \left(\frac{x}{\beta} \right) + (1-x) \log \left(\frac{1-x}{1-\beta} \right) \right)$$

is strictly convex with minimum β and hence, $f|_{[\beta, 1]}$ is strictly increasing. Thus, (33) implies that for all $\hat{\theta} \geq \theta_s^- + \delta_s/2$, if $\zeta_{I_s^-} \leq \theta_s^- + \delta_s/2$

$$T_{I_s^-}(W(Z, \hat{\theta}), \beta) = f(W(Z, \hat{\theta})) \geq f(W(Z, \theta_s^- + \delta_s/2)) = T_{I_s^-}(W(Z, \theta_s^- + \delta_s/2), \beta)$$

and hence,

$$\begin{aligned} \mathbb{P}(\Omega_s^-) &\leq \mathbb{P} \left(\Omega_s^- \cap \left\{ \zeta_{I_s^-} \leq \theta_s^- + \frac{\delta_s}{2} \right\} \right) + \mathbb{P} \left(\zeta_{I_s^-} > \theta_s^- + \frac{\delta_s}{2} \right) \\ &\leq \mathbb{P} \left(T_{I_s^-}(W(Z, \theta_s^- + \delta_s/2), \beta) \leq \frac{\left(q + \sqrt{2 \log(2e/\lambda_s)} \right)^2}{2} \right) + \mathbb{P} \left(\zeta_{I_s^-} > \theta_s^- + \frac{\delta_s}{2} \right) \\ &\leq 2 \exp \left(-\frac{\left(\sqrt{2n\lambda_s} \xi_{F,\beta}(\delta_s/2) - q - \sqrt{2 \log(2e/\lambda_s)} \right)_+^2}{2} \right) \\ &\quad + 2 \exp(-n\lambda_s \xi_{F,\beta}(\delta_s/2)^2), \end{aligned}$$

where the last inequality follows from Theorems A.2 and A.3. Hence,

$$\mathbb{P}(\Omega_s) \leq 1 - (1 - \mathbb{P}(\Omega_s^+))(1 - \mathbb{P}(\Omega_s^-)) \leq 1 - \gamma_{n,s},$$

with $\gamma_{n,s}$ as in (24). For $s = 1, \dots, S-1$ define the random variables

$$X_s(\omega) = \begin{cases} 0 & \text{if } \omega \in \Omega_s, \\ 1 & \text{otherwise.} \end{cases}$$

Observe that $X_s = 1$ implies that any function $\hat{\vartheta} \in \Sigma$ with $T_n(W(Z, \vartheta), \beta) \leq q$ has at least one change point on I_s . Since I_1, \dots, I_{S-1} are pairwise disjoint this implies $\hat{S}(q) - 1 \geq \sum_{s=1}^{S-1} X_s$. Therefore

$$\mathbb{P}(\hat{S}(q) \geq S) \geq \mathbb{P}\left(\sum_{s=1}^{S-1} X_s \geq S-1\right) = \prod_{s=1}^{S-1} (1 - \mathbb{P}(\Omega_s)) = \prod_{s=1}^{S-1} \gamma_{n,s}.$$

□

Proof of Corollary 1.2. Let $\gamma_{n,s}(q)$ be as in (24), Ξ, Λ as in (10), and $\gamma_n(q)$ be defined as $\gamma_n(q) = \min_{1 \leq s \leq S-1} \gamma_{n,s}(q)$. Then

$$\begin{aligned} \gamma_n(q) &\geq \left[1 - 2 \exp\left(-\frac{\left(2\sqrt{n\Lambda/2}\Xi - q - \sqrt{2\log(2e/\Lambda)}\right)_+^2}{2} \right) - 2 \exp(-n\Lambda\Xi^2) \right]^2 \\ &= \left[1 - 2 \exp\left(-\left(\sqrt{n\Lambda}\Xi - q/\sqrt{2} - \sqrt{\log(2e/\Lambda)}\right)_+^2 \right) - 2 \exp(-n\Lambda\Xi^2) \right]^2. \end{aligned} \quad (34)$$

From Theorem 2.1 it follows that

$$\mathbb{P}(\hat{S}(q) < S) \leq 1 - \prod_{s=1}^{S-1} \gamma_{n,s}(q) \leq 1 - \gamma_n(q)^{S-1}.$$

Using the inequality $(1-x)^m \geq 1 - mx$ for all $x \in (0, 1)$ and $m \in \mathbb{N}$ and (34) it follows that

$$\begin{aligned} \mathbb{P}(\hat{S}(q) < S) &\leq 4(S-1) \left[\exp\left(-\left(\sqrt{n\Lambda}\Xi - q/\sqrt{2} - \sqrt{\log(2e/\Lambda)}\right)_+^2 \right) + \exp(-n\Lambda\Xi^2) \right] \\ &\leq 4(S-1) e^{-n\Lambda\Xi^2} \left[e^{2\sqrt{n\Lambda}\Xi\left(q/\sqrt{2} + \sqrt{\log(2e/\Lambda)}\right)} + 1 \right], \end{aligned}$$

where the last inequality comes from the fact that $a^2 - (a-b)^2 \leq 2ab$, with $a = \sqrt{n\Lambda}\Xi$ and $b = q/\sqrt{2} + \sqrt{\log(2e/\Lambda)}$. The result follows from the fact that $S \leq \Lambda^{-1}$ □

Proof of Theorem 2.2. From the proof of Corollary 1.2 we get the following bound

$$\begin{aligned} & \mathbb{P}(\hat{S}(q) < S) \\ & \leq 4\Lambda_n^{-1} \left[\exp \left(- \left(\sqrt{n\Lambda_n} \Xi_n - q_n/\sqrt{2} - \sqrt{\log(2e/\Lambda_n)} \right)_+^2 \right) + \exp(-n\Lambda_n \Xi_n^2) \right] \\ & = 4 [\exp(-\Gamma_{1,n}) + \exp(-\Gamma_{2,n})] \end{aligned}$$

with $\Gamma_{1,n} = \left(\sqrt{n\Lambda_n} \Xi_n - q_n/\sqrt{2} - \sqrt{\log(2e/\Lambda_n)} \right)_+^2 + \log \Lambda_n$ and $\Gamma_{2,n} = n\Lambda_n \Xi_n^2 + \log \Lambda_n$.

Then a sufficient condition for $\mathbb{P}(\hat{S}(q) < S) \rightarrow 0$ is that $\Gamma_{1,n} \rightarrow \infty$ and $\Gamma_{2,n} \rightarrow \infty$ as $n \rightarrow \infty$.

Cases 1 and 2: If $\liminf \Lambda_n > 0$, then a sufficient condition for $\Gamma_{1,n} \rightarrow \infty$ is that

$$\sqrt{n\Lambda_n} \Xi_n - q_n/\sqrt{2} \rightarrow \infty.$$

This holds if $\sqrt{n\Xi_n}/q_n \rightarrow \infty$. Moreover, if this is the case then $\Gamma_{2,n} \rightarrow \infty$ as $n \rightarrow \infty$ and the proof is finished.

Case 3: If $\Lambda_n \rightarrow 0$, assume that $\sqrt{n\Lambda_n} \Xi_n \geq (2 + \epsilon_n) \sqrt{-\log \Lambda_n}$ for a sequence ϵ_n such that $\epsilon_n \sqrt{-\log \Lambda_n}/q_n \rightarrow \infty$. Using the inequality $\sqrt{x+y} - \sqrt{x} \leq y/(2\sqrt{x})$ for $x, y \geq 0$ we obtain

$$\begin{aligned} \Gamma_{1,n} & \geq \left((2 + \epsilon_n) \sqrt{-\log \Lambda_n} - \frac{q_n}{\sqrt{2}} - \sqrt{1 + \log 2 - \log \Lambda_n} \right)_+^2 + \log(\Lambda_n) \\ & \geq \left((1 + \epsilon_n) \sqrt{-\log \Lambda_n} - \frac{q_n}{\sqrt{2}} - \frac{1 + \log 2}{2\sqrt{-\log \Lambda_n}} \right)_+^2 + \log(\Lambda_n) \\ & \geq \left(\epsilon_n \sqrt{-\log \Lambda_n} - \frac{q_n}{\sqrt{2}} - \frac{1 + \log 2}{2\sqrt{-\log \Lambda_n}} \right)_+^2 \end{aligned}$$

where the last inequality comes from the fact that $(a+b)^2 - a^2 \geq b^2$, for $a, b \geq 0$. A sufficient condition for $\Gamma_{1,n} \rightarrow \infty$ is then that $\epsilon_n \sqrt{-\log \Lambda_n}/q_n \rightarrow \infty$, as it was assumed. Note that $\sqrt{n\Lambda_n} \Xi_n \geq (2 + \epsilon_n) \sqrt{-\log \Lambda_n}$ implies

$$\begin{aligned} \Gamma_{2,n} & \geq [1 - (2 + \epsilon_n)^2] \log \Lambda_n \\ & = (-3 - 4\epsilon_n - \epsilon_n^2) \log \Lambda_n \end{aligned}$$

which goes to infinity as by definition $\liminf_n \epsilon_n \geq 0$. □

Proof of Theorem 2.3. As in the proof of Theorem 2.1, define S disjoint intervals

$$I_s = (\tau_s - \epsilon_n, \tau_s + \epsilon_n) \subseteq [0, 1],$$

and define I_s^+ , I_s^- , θ_s^+ and θ_s^- accordingly. Now assume an estimator $\hat{\vartheta}$ of ϑ , with estimated number of segments \hat{S} , such that $T_n(Z, \hat{\vartheta}) \leq q$ and

$$\max_{0 \leq s \leq S-1} \min_{0 \leq l \leq \hat{S}-1} |\hat{\tau}_l - \tau_s| > \epsilon_n.$$

In other words, there exists $0 \leq s \leq S-1$ such that $|\hat{\tau}_l - \tau_s| > \epsilon_n$ for all $0 \leq l \leq \hat{S}-1$, i.e. $\hat{\theta}$ does not have a change point in the interval I_s . Then, as in the proof of Theorem 2.1,

$$\begin{aligned} & \mathbb{P} \left(\exists \hat{\theta} \in \Sigma : T_n(Z, \hat{\theta}) \leq q \text{ and } \max_{0 \leq s \leq S-1} \min_{0 \leq l \leq \hat{S}-1} |\hat{\tau}_l - \tau_s| > \epsilon_n \right) \\ & \leq \mathbb{P} \left(\exists \hat{\theta} \in \mathbb{R} \text{ and some } s : \sqrt{2T_{I_s^+}(W(Z, \hat{\theta}), \beta)} - \sqrt{2 \log \frac{\epsilon n}{\epsilon_n}} \leq q \text{ and} \right. \\ & \quad \left. \sqrt{2T_{I_s^-}(W(Z, \hat{\theta}), \beta)} - \sqrt{2 \log \frac{\epsilon n}{\epsilon_n}} \leq q \right) \end{aligned}$$

Finally, the assertion follows by replacing λ_s by ϵ_n in the proof of Theorem 2.1. \square

References

Astola, J. T. and T. G. Campbell (1989). On computation of the running median. *IEEE Trans. Acoust. 37*(4), 572–574.

Aue, A., R. C. Y. Cheung, T. C. M. Lee, and M. Zhong (2014). Segmented model selection in quantile regression using the minimum description length principle. *J. Am. Stat. Assoc. 109*(507), 1241–1256.

Aue, A., R. C. Y. Cheung, T. C. M. Lee, and M. Zhong (2017). Piecewise quantile autoregressive modeling for nonstationary time series. *Bernoulli 23*(1), 1–22.

Bai, J. and P. Perron (1998). Estimating and testing linear models with multiple structural changes. *Econometrica 66*(1), 47–78.

Behr, M. (2018). *Finite Alphabet Blind Separation*. Ph. D. thesis, University of Goettingen.

Behr, M., C. Holmes, and A. Munk (2018). Multiscale blind source separation. *Ann. Stat. 46*(2), 711–744.

Bellman, R. (1954). The theory of dynamic programming. *Bull. Amer. Math. Soc. 60*(6), 503–515.

Belloni, A. and V. Chernozhukov (2011). L1-penalized quantile regression in high-dimensional sparse models. *Ann. Stat. 39*(1), 82–130.

Boysen, L., A. Kempe, V. Liebscher, A. Munk, and O. Wittich (2009). Consistencies and rates of convergence of jump-penalized least squares estimators. *Ann. Stat. 37*(1), 157–183.

Cai, Z. and H. Xiong (2012). Partially varying coefficient instrumental variables models. *Stat. Neerl. 66*(2), 85–110.

Celisse, A., G. Marot, M. Pierre-Jean, and G. J. Rigaill (2018). New efficient algorithms for multiple change-point detection with reproducing kernels. *Comput. Stat. Data Anal.* 128, 200–220.

Chung, S.-H., O. S. Anderson, and V. V. Krishnamurthy (Eds.) (2007). *Biological Membrane Ion Channels: Dynamics, Structure, and Applications*. Biological and Medical Physics, Biomedical Engineering. New York: Springer-Verlag.

Cribben, I. and Y. Yu (2017). Estimating whole-brain dynamics by using spectral clustering. *J. R. Stat. Soc. Ser. C Appl. Stat.* 66(3), 607–627.

Davies, L., C. Höhenrieder, and W. Krämer (2012). Recursive computation of piecewise constant volatilities. *Comput. Stat. Data Anal.* 56(11), 3623–3631.

Du, C., C.-L. M. Kao, and S. C. Kou (2016). Stepwise signal extraction via marginal likelihood. *J. Am. Stat. Assoc.* 111(513), 314–330.

Dümbgen, L. and A. Kovac (2009). Extensions of smoothing via taut strings. *Electron. J. Stat.* 3(0), 41–75.

Dümbgen, L. (1998). New goodness-of-fit tests and their application to nonparametric confidence sets. *Ann. Stat.* 26(1), 288–314.

Dümbgen, L. and V. G. Spokoiny (2001). Multiscale testing of qualitative hypotheses. *Ann. Stat.* 29(1), 124–152.

Dümbgen, L. and G. Walther (2008). Multiscale inference about a density. *Ann. Stat.* 36(4), 1758–1785.

Eilers, P. H. C., D. Menezes, and R. X (2005). Quantile smoothing of array CGH data. *Bioinformatics* 21(7), 1146–1153.

Fearnhead, P. (2006). Exact and efficient Bayesian inference for multiple changepoint problems. *Stat. Comput.* 16(2), 203–213.

Fearnhead, P. and G. Rigaill (2017). Changepoint detection in the presence of outliers. *J. Am. Stat. Assoc.*, 1–15.

Frick, K., A. Munk, and H. Sieling (2014). Multiscale change point inference. *J. R. Stat. Soc. Series B Stat. Methodol.* 76(3), 495–580.

Fryzlewicz, P. (2014). Wild binary segmentation for multiple change-point detection. *Ann. Stat.* 42(6), 2243–2281.

Fryzlewicz, P. (2018). Tail-greedy bottom-up data decompositions and fast multiple change-point detection. *Ann. Stat.* 46(6B), 3390–3421.

Futschik, A., T. Hotz, A. Munk, and H. Sieling (2014). Multiscale DNA partitioning: Statistical evidence for segments. *Bioinformatics* 30(16), 2255–2262.

Gnanasambandam, R., M. S. Nielsen, C. Nicolai, F. Sachs, J. P. Hofgaard, and J. K. Dreyer (2017). Unsupervised idealization of ion channel recordings by minimum description length: Application to human PIEZO1-channels. *Front. Neuroinform.* 11.

Harchaoui, Z. and C. Lévy-Leduc (2010). Multiple change-point estimation with a total variation penalty. *J. Am. Stat. Assoc.* 105(492), 1480–1493.

Haynes, K., P. Fearnhead, and I. A. Eckley (2017). A computationally efficient nonparametric approach for changepoint detection. *Stat. Comput.* 27(5), 1293–1305.

Jeng, X. J., T. T. Cai, and H. Li (2010). Optimal sparse segment identification with application in copy number variation analysis. *J. Am. Stat. Assoc.* 105(491), 1156–1166.

Jónás, A., T. Taus, C. Kosiol, C. Schlötterer, and A. Futschik (2016). Estimating the effective population size from temporal allele frequency changes in experimental evolution. *Genetics* 204(2), 723–735.

Kempe, A., V. Liebscher, and G. Winkler (2008). Complexity Penalized M-Estimation AU - Friedrich, F. *J. Comput. Graph. Stat.* 17(1), 201–224.

Killick, R., P. Fearnhead, and I. A. Eckley (2012). Optimal detection of changepoints with a linear computational cost. *J. Am. Stat. Assoc.* 107(500), 1590–1598.

Koenker, R. (2005). *Quantile Regression*. Cambridge University Press.

Li, H., A. Munk, and H. Sieling (2016). FDR-control in multiscale change-point segmentation. *Electron. J. Stat.* 10(1), 918–959.

Li, Y. and J. Zhu (2007). Analysis of array CGH data for cancer studies using fused quantile regression. *Bioinformatics* 23(18), 2470–2476.

Liu, B., C. D. Morrison, C. S. Johnson, D. L. Trump, M. Qin, J. C. Conroy, J. Wang, and S. Liu (2013). Computational methods for detecting copy number variations in cancer genome using next generation sequencing: Principles and challenges. *Oncotarget* 4(11), 1868–1881.

Machado, J. A. F. and J. M. C. S. Silva (2005). Quantiles for counts. *J. Am. Stat. Assoc.* 100(472), 1226–1237.

Massart, P. (1990). The tight constant in the Dvoretzky-Kiefer-Wolfowitz inequality. *The Annals of Probability* 18(3), 1269–1283.

Matteson, D. S. and N. A. James (2014). A nonparametric approach for multiple change point analysis of multivariate data. *J. Am. Stat. Assoc.* 109(505), 334–345.

Niu, Y. S. and H. Zhang (2012). The screening and ranking algorithm to detect DNA copy number variations. *Ann. Appl. Stat.* 6(3), 1306–1326.

Olshen, A. B., E. S. Venkatraman, R. Lucito, and M. Wigler (2004). Circular binary segmentation for the analysis of array-based DNA copy number data. *Biostatistics (Oxford, England)* 5(4), 557–572.

Pein, F., H. Sieling, and A. Munk (2017). Heterogeneous change point inference. *J. R. Stat. Soc. Series B Stat. Methodol.* 79(4), 1207–1227.

Preuss, P., R. Puchstein, and H. Dette (2015). Detection of multiple structural breaks in multivariate time series. *J. Am. Stat. Assoc.* 110(510), 654–668.

Rosenberg, A. and J. Hirschberg (2007). V-measure: A conditional entropy-based external cluster evaluation measure. In *Proceedings of the 2007 Joint Conference on Empirical Methods in Natural Language Processing and Computational Natural Language Learning*, Prague, pp. 410–420.

Ruggieri, E. (2018). A pruned recursive solution to the multiple change point problem. *Comput. Stat.* 33(2), 1017–1045.

Russell, B. and D. Rambaccussing (2018). Breaks and the statistical process of inflation: The case of estimating the ‘modern’ long-run Phillips curve. *Empir. Econ.*, 1–21.

Sakmann, B. and E. Neher (1995). *Single-Channel Recording, 2nd Edition*. Springer.

Shen, H. (2016). The detection and empirical study of variance change points on housing prices-taking Wuhan City commodity prices as an example. *Journal of Mathematical Finance* 06, 699.

Siegmund, D. (2013). Change-points: From sequential detection to biology and back. *Seq. Anal.* 32(1), 2–14.

Spokoiny, V. (2009). Multiscale local change point detection with applications to value-at-risk. *Ann. Stat.* 37(3), 1405–1436.

Tibshirani, R. and P. Wang (2008). Spatial smoothing and hot spot detection for CGH data using the fused lasso. *Biostatistics* 9(1), 18–29.

Tsybakov, A. B. (2009). *Introduction to Nonparametric Estimation*. Springer Series in Statistics. New York: Springer-Verlag.

Virji, M. (2009). Pathogenic neisseriae: Surface modulation, pathogenesis and infection control. *Nat. Rev. Microbiol.* 7(4), 274–286.

Wald, A. and J. Wolfowitz (1940). On a test whether two samples are from the same population. *Ann. Math. Stat.* 11(2), 147–162.

Wang, G., C. Zou, and G. Yin (2018). Change-point detection in multinomial data with a large number of categories. *Ann. Stat.* 46(5), 2020–2044.

Zhang, N. R. and D. O. Siegmund (2007). A modified Bayes information criterion with applications to the analysis of comparative genomic hybridization data. *Biometrics* 63(1), 22–32.

Zou, C., G. Yin, L. Feng, and Z. Wang (2014). Nonparametric maximum likelihood approach to multiple change-point problems. *Ann. Stat.* 42(3), 970–1002.